

Report

1. Numerical Simulation Of Laminar And Turbulent Flow Through Pipe.
2. Steady State Jet Impingement With Different Plenum Configuration On Flat Plate.

Summer Internship

May,15th- June 30th,2024

Steam-Power Lab, IIT Bombay



Department of
Mechanical Engineering
Indian Institute of Technology Bombay

Submitted by-Karan Shukla

Department of Chemical Engineering
Indian Institute of Technology, Jammu,

Supervisor- Prof. RP Vedula

Department of Mechanical Engineering
Indian Institute of Technology, Bombay

1-Numerical Simulation of Steady State Laminar Flow through Pipe.

1.1 Introduction:

The concepts of Fluid Mechanics and Heat Transfer finds huge application in transport phenomena in industries. Among those applications the flow through the pipe is the most common application of momentum and heat transfer unit operation. In this section of the report, a numerical simulation of Laminar flow through the pipe has been extensively discussed primarily focusing on calculation of a heat transfer non-dimensional number, Nusselt Number (Nu) and fluid mechanics parameter, friction factor (f).

Laminar flow is a flow in which the streamlines are parallel to one another. The laminar and turbulent nature of fluid flow is defined based on Reynolds Number (Re). For $Re < 2300$, the flow through the pipe is considered as laminar. The Re is defined as the ratio of inertial forces to the viscous forces as mentioned in equation 1.1(a).

$$Re = \frac{\rho u D}{\mu} \quad 1.1(a)$$

The geometry of the pipe is shown in figure 1.1(a).

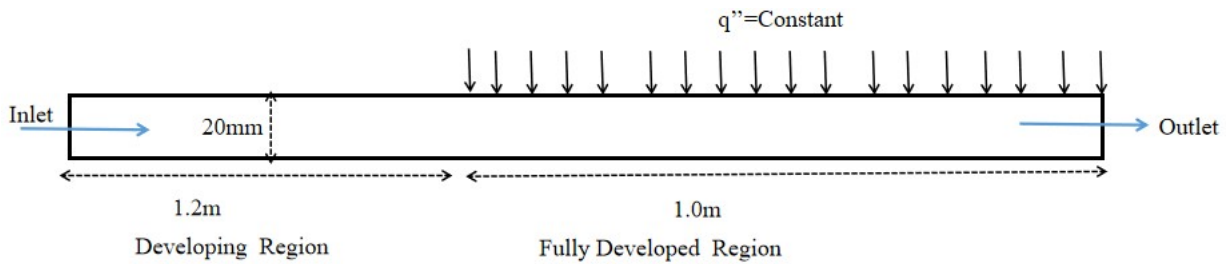


Figure 1.1(a): Geometry of pipe is illustrated.

The L_d denotes the length of developing region and D is the diameter of the pipe through which fluid flow occurs. The ratio of L_d and D is the function of Re which is expressed in equation 1.1(b).

$$\frac{L_d}{D} = 0.06 Re \quad 1.1(b)$$

$$L_d = 0.06 \times 100 \times 0.02$$

$$L_d = 0.12m \text{ (Required to become fully Developed Flow)}$$

Entrance length of 1.2 m is given as developing region in the geometry which is too good for the fluid to become fully developed.

Fluid Properties	Values
Density(Kg/m ³)	998.2
Thermal Conductivity(W/m K)	0.6
Specific Heat (J/Kg K)	4182
Dynamic Viscosity(Pa-s)	0.001003
Re	100

Table 1.1(a): Fluid properties

1.2 Methodology:

Once the geometry is prepared and the control volume is created, the next step is to create the computational mesh for the 3d pipe. Meshing is the process in which the computational domain, i.e., the control volume is divided into very small sub-volumes. Within these sub-volumes, equations of fluid dynamics and heat transfer are solved to obtain the behavior of a fluid flow and heat transfer in and around an object. The process of meshing is extremely critical and great care needs to be taken to create a mesh in order to capture the correct fluid flow behavior.

Mesh Details	Values
Mesh Type	HEX
Element size(mm)	1

Boundary conditions	Data
Inlet velocity(m/s)	0.05
Inlet temperature(K)	300
Outlet	$P_g=0$

Table 1.2 (a): Mesh details are illustrated.

Wall Flux(W/m ² K)	1000
-------------------------------	------

Table 1.2(b): Boundary conditions are illustrated

$$Re = \frac{\rho u d}{\mu}$$

$$100 = \frac{998.2 \times u \times 0.02}{0.00103}$$

$$u = 0.005 \text{ m/s}$$

The total number of nodes and number of elements are 7,86,114 and 7,12,800 respectively. The simulation is run for 1000 iterations and the solutions converges at 268th iteration. The obtained convergence chart is shown in table 1.2(c). ANSYS FLUENT provides four segregated types of algorithms: SIMPLE, SIMPLEC, PISO. The scheme used for simulation is Simple. These schemes are referred to as the pressure-based segregated algorithm. Steady-state calculations will generally use SIMPLE or SIMPLEC, while PISO is recommended for transient calculations. PISO may also be useful for steady-state and transient calculations on highly skewed meshes. Using the Coupled algorithm enables full pressure-velocity coupling, hence it is referred to as the pressure-based coupled algorithm.

Iterations	268
continuity	9.8767e-07
x-velocity	3.2703e-10
y-velocity	7.3715e-10
z-velocity	1.7988e-08
energy	7.0230e-12

Table 1.2(c): Convergence chart

1.3 Results and Discussion:

The flow velocity profile in a fully developed laminar flow inside a circular pipe is parabolic. Hagen-Poiseuille flow is the well-known term for this. Because of the viscous friction between the fluid and the pipe wall, the fluid velocity is highest near the centre of the pipe and gradually drops towards the edges (pipe wall). In laminar flow within a pipe, pressure drop is an important component to take into account. This is the pressure differential between two locations along the pipe, which is frequently brought on by variations in pipe friction or height. The pressure drop in the pipe is shown in figure 1.3(a).

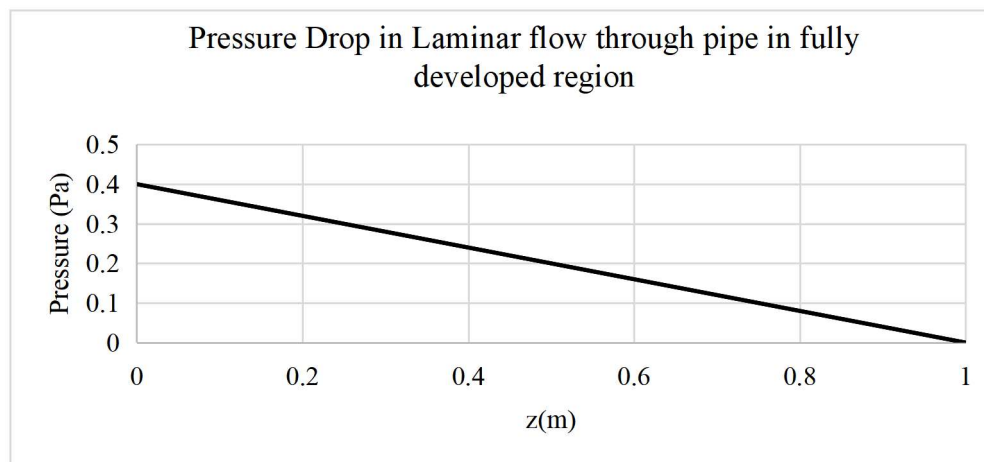


Figure 1.3(a): Pressure drop in laminar pipe in fully developed region .

$$f_{simulation} = \frac{2d}{\rho u^2} \frac{\Delta P}{L} \quad 1.3(a)$$

$$= \frac{2 \times 0.02 \times 0.4}{998.2 \times 0.005^2}$$

$$= 0.641$$

$$f_{Literature} = \frac{64}{Re} \quad 1.3(b)$$

$$= \frac{64}{100}$$

$$= 0.64$$

The deviation in friction factor is **0.18%**.

The heat transfer in the pipe is fundamentally understood with calculating Nu within the pipe. The Nu can be calculated based on wall temperature and bulk temperature within the pipe. The wall temperature can be calculated along the length of the pipe by drawing a line at the fluid and wall interface and bulk temperature can be calculated using mass weighted average corresponding to each plane drawn along the axis of the pipe. The wall is at constant heat flux of $1000 \text{ W/m}^2\text{K}$. The Nu can be expressed in terms of wall and bulk temperature is given in equation 1.3(c) and 1.3(d).

$$Nu = \frac{h d}{k} \quad 1.3(c)$$

$$h = \frac{q''}{T_{wall} - T_{bulk}} \quad 1.3(d)$$

Both the wall and bulk temperature monotonously increase along the axis which is plotted in figure 1.3(b). The Nu is calculated at each z and then Nu is plotted in figure 1.3(c).

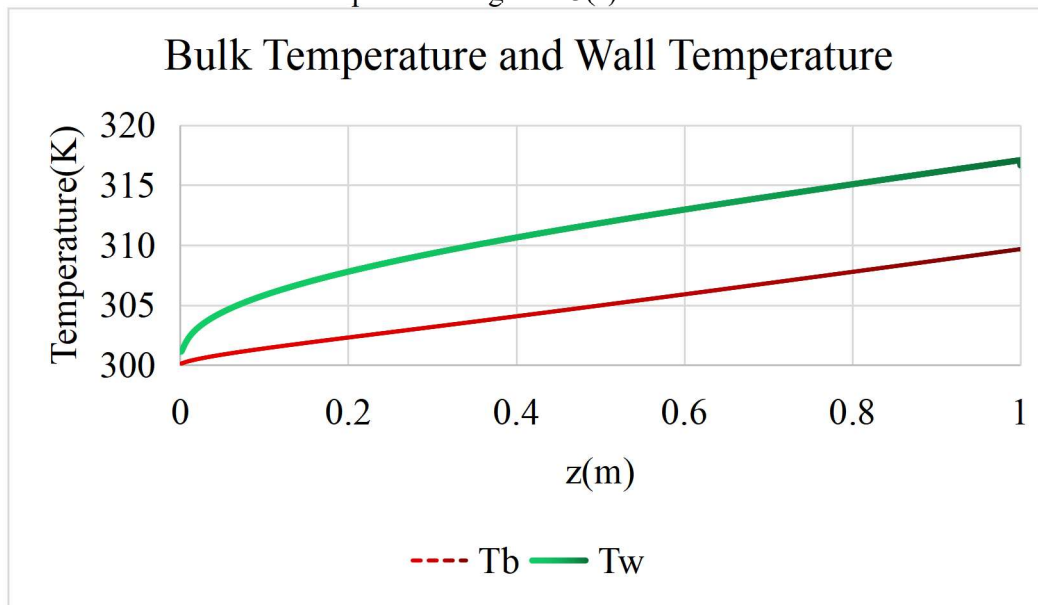


Figure 1.3(b): Wall and Bulk Temperature monotonically increasing in Fully developed region.

Sample Calculation:

At $z = 0.5\text{m}$ (Starting from Fully developed region), $T_{wall} = 311.828064\text{K}$ and $T_{bulk} = 304.968 \text{ K}$

Heat transfer coefficient $= h = \frac{q''}{(T_{wall} - T_{bulk})} = 146 \text{ W/m}^2\text{K}$

$$Nu = \frac{h d}{k} = 4.86$$

The Nu is plotted against the axial location in figure 1.3(c). The Nu for laminar flow through a pipe subjected to constant heat flux is 4.36. This value can be compared with the result obtained after performing numerical simulation.

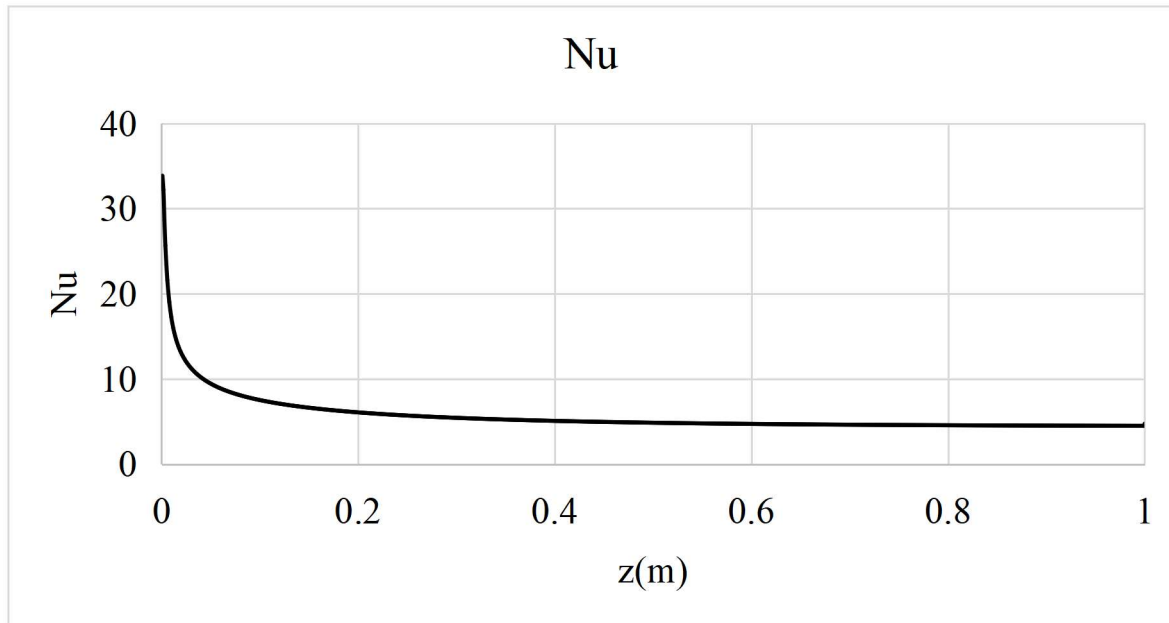


Figure 1.3(c): Nu for constant heat flux at walls is 4.49 obtained from Numerical Simulation with deviation of 2.8% from literature.

The deviation from literature of the Nu is **2.8%**.

2: Numerical Simulation of Steady State Turbulent Flow through Pipe

2.1 Introduction:

This section will focus on numerically simulating turbulent flow through a pipe with a Reynolds number of 20,000. The primary objective is to gain the ability of simulating turbulent models in Fluent by creating proper mesh and establishing correct boundary conditions with suitable models and scheme to efficiently converge the solution. The simulation involves modelling a three-dimensional pipe subjected to a continuous heat flux at the walls of the fully developed flow regions. The geometry can be duplicated for running the turbulent flow model also. Since the same developing region length is sufficient to establish a fully developed velocity profile after L_d . The fluid properties such as density, viscosity, thermal conductivity and specific heat is same as taken for laminar flow through pipe simulation. Since the flow is now turbulent therefore the Re must be higher than 2300. For the simulation purpose $Re = 20,000$ has been taken which can cause the flow to be turbulent.

2.2 Methodology:

A wall function is necessary to precisely predict the flow within the boundary layer. The boundary layer refers to the narrow zone adjacent to a wall where there is a significant change in velocity perpendicular to the wall. This change in velocity ranges from zero at the wall to almost the same velocity as the main flow at a specific distance away from the wall. A turbulent boundary layer consists of a slender viscous sub-layer adjacent to the wall, a transition layer (buffer zone), and the turbulent boundary layer. The total number of nodes and elements are 7,86,114 and 7,12,800 respectively after generating the mesh as per the details given in figure table 2.2(a).

Mesh Details	Values
Mesh Type	HEX
Element size(mm)	1.5
Y+	1
ΔY_1 (mm)	0.0356741
Growth rate	1.2
Maximum Layers	10

Table 2.2(a): Meshing details are shown.

Calculation for Y+:

Firstly, we should calculate the Reynolds number for our model based on the characteristic scales of our geometry such that:

$$Re = \frac{\rho u d}{\mu}$$

where ρ and μ are the fluid density and viscosity respectively, U is the free stream velocity, and d is the pipe diameter.

The definition of the Y^+ value is such that:

$$Y^+ = \frac{\rho u \Delta Y_1}{\mu}$$

The target Y^+ value and fluid properties are known a priori, so we need to calculate the frictional velocity, U which is defined as:

$$u = \sqrt{\frac{\tau_w}{\rho}}$$

The wall shear stress, τ_w can be calculated from skin friction coefficient, C_f , such that:

$$\tau_w = \frac{1}{2} C_f \rho u^2$$

The ambiguity in calculating ΔY_1 surrounds the value for C_f . Empirical results have been used to provide an estimate to this value:

For internal flows: $C_f = 0.079 Re^{-0.25}$

Taking $Y^+ = 1$ { When the viscous sub-layer needs to be captured in cases like transitional flow, separation, heat transfer, frictional drag prediction etc., the first cell has to be located within the viscous sub-layer and the y^+ should be less than 1. }

$u = 1\text{m/s}$, $d = 0.02\text{m}$, $\rho = 998.2\text{ Kg/m}^3$ and $\mu = 0.00103\text{Pa-s}$

$\Delta Y_1 = 0.0356741\text{ mm}$

From a computational fluid dynamics (CFD) perspective, it is crucial to generate a mesh or grid that can precisely forecast the velocity gradient within the boundary layer. In the case of turbulent flows, it is desirable for the first cell from the wall to be located within the extremely narrow viscous sub-layer. Y-plus (y^+) is crucial element in the context of wall functions. Y^+ represents the dimensionless distance from the wall to the first node away from the wall

Boundary conditions	Data
Inlet velocity(m/s)	1
Inlet temperature(K)	300
Outlet	$P_g=0$
Wall Flux(W/m ² K)	1000

Table 2.2(b): Boundary conditions for the geometry.

The inlet velocity can be calculated based on Re . Since the $Re = 20,000$ for the flow therefore following calculations can be performed to obtain the inlet velocity.

$$Re = \frac{\rho u d}{\mu}$$

$$20,000 = \frac{998.2 \times u \times 0.02}{0.00103}$$

$$u = 1 \text{ m/s}$$

The RNG-K epsilon model is used to simulate the system with Enhanced wall treatment. The RNG model was developed using Re-Normalization Group (RNG) methods to normalize the Navier-Stokes equations, to account for the effects of smaller scales of motion. The SIMPLE scheme is used to run the simulation. The boundary conditions are provided in table 2.2(b). The solution converges at 390 iteration with initial number of iteration given = 1000.

Convergence: All the residuals which includes continuity, momentum, energy, k and epsilon are lesser are found to converge at 390 iterations with convergence reach of less than 10^{-8} .

2.3 Results and Discussion:

There will be a pressure drop when fluid passes through a pipe because of flow resistance. Additionally, a change in elevation between the pipe's start and termination could result in a pressure gain or loss. It is vital to compute a pressure drop, often expressed in fluid head, for each object that alters pressure in order to determine the pressure loss in a pipe. In order to compute the friction factor equation 2.3(a) and 2.3(b) is used.

$$f_{simulation} = \frac{2d \Delta P}{\rho u^2 L} \quad 2.3(a)$$

$$f_{literature} = \frac{0.316}{Re^{0.25}} \quad 2.3(b)$$

The pressure drop in the pipe is plotted in figure 2.3(a).

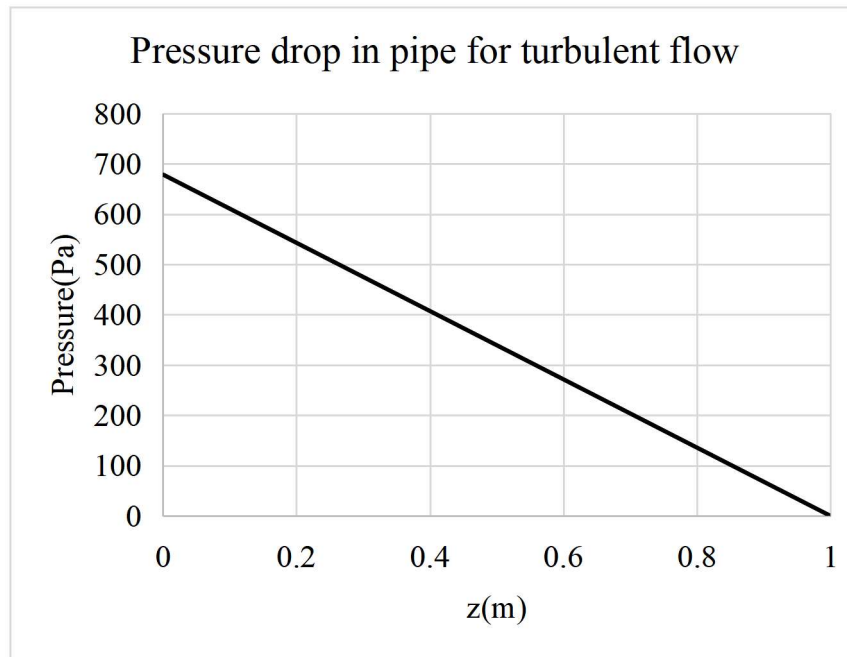


Figure 2.3(a): Pressure drop along the length of pipe

The friction factor calculated from Numerical simulation and from existing correlation is tabulated below in table 2.3(a) along with % deviation.

$$f_{simulation} = \frac{2d \Delta P}{\rho u^2 L}$$

$$= \frac{2 \times 0.02 \times 678}{998.2 \times 1^2}$$

$$= 0.0272$$

$$f_{literature} = \frac{0.316}{Re^{0.25}}$$

$$= \frac{0.316}{20,000^{0.25}}$$

$$= 0.02657$$

	Simulation	Literature	Deviation
f	0.0272	0.02657	2.28%

Table 2.3(a): Friction factor comparison

The bulk temperature and wall temperature along the axis is calculated by applying similar steps as done for laminar flow through pipe. A similar trend will be observed in the plots of bulk and wall temperature. Both temperature will monotonously increases along the axis. Bulk temperature always being lesser than wall temperature as shown in figure 2.3(b).

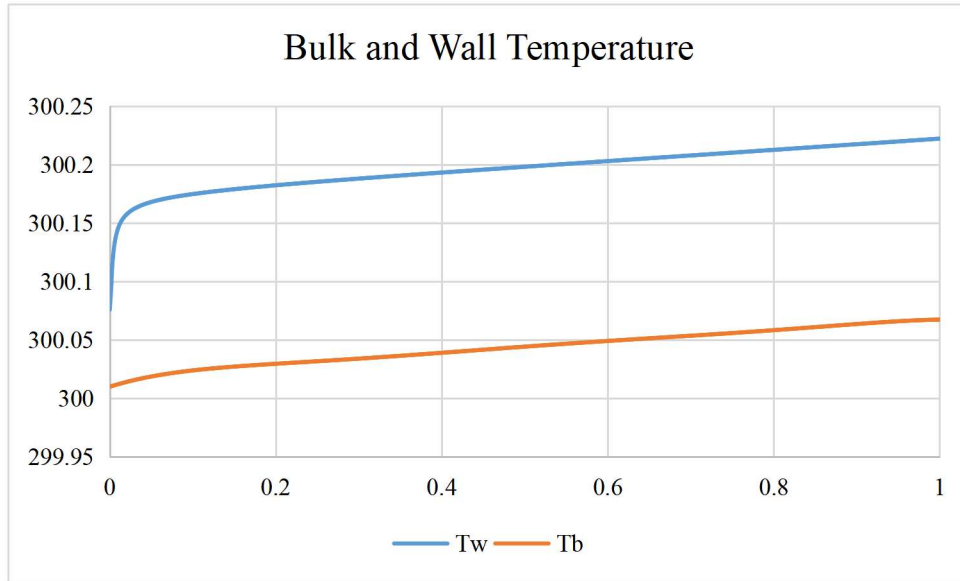


Figure 2.3(b): Wall and Bulk Temperature monotonically increasing in Fully developed region.

Sample Calculation for Nu:

At $z = 0.5\text{m}$ (Starting from fully developed region) , $T_{wall} = 300.19812\text{ K}$, $T_{bulk} = 300.044301\text{ K}$

$$h = \frac{q''}{T_{wall} - T_{bulk}} = 6501.132326 \quad \text{W/m}^2\text{K}$$

$$Nu = \frac{hd}{k} = 216.70$$

The Nu plotted in figure 2.3(c) can be bench marked by Gnielinski correlation which are valid for Reynolds numbers range from $2300 \leq Re \leq 5 \times 10^6$ for a range of Prandtl number $0.5 \leq Pr \leq 1000$. The Pr here is 7.1791 which can be calculated using equation 2.3(c). Therefore the correlation for $Pr = 7.1791$ is given in equation 2.3(d).

$$Pr = \frac{c_p \mu}{k} \quad 2.3(c)$$

$$Nu = \frac{(f/8)(Re-1000)Pr}{1+12.7(f/8)^2(Pr^{2/3}-1)} \quad 2.3(d)$$

$$= \frac{(0.027179/8)(20,000-1000)7.1791}{1+12.7(0.027179/8)^2(7.1791^{2/3}-1)}$$

$$= 153.72$$

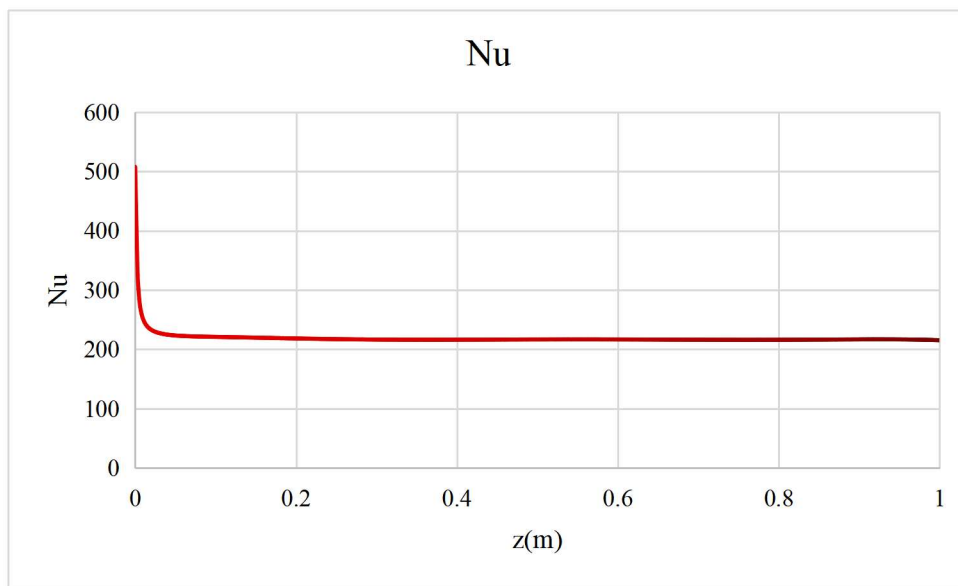


Figure 2.3(c): Nu for constant heat flux at walls is 153.72 from equation 2.3(d) and 215.38 obtained from Numerical Simulation with deviation of **28.62%** .

3: Numerical Simulation of Steady State Jet Impingement on Flat Plate through open nozzle.

3.1 Introduction:

This study is a computational analysis that investigates the influence of geometric parameters on heat transfer in a three-dimensional jet impingement on a flat plate with a nozzle diameter of d (20 mm) as shown in figure 3.1(a). The fluid motion is characterized by turbulence when the Reynolds number is 23,000. The distance between the nozzle and the bottom wall plate is H . The geometric dimensions are presented in table 3.1 (a), whereas the properties of the fluid are displayed in table 3.1 (b). The total length of impinging plate is L .

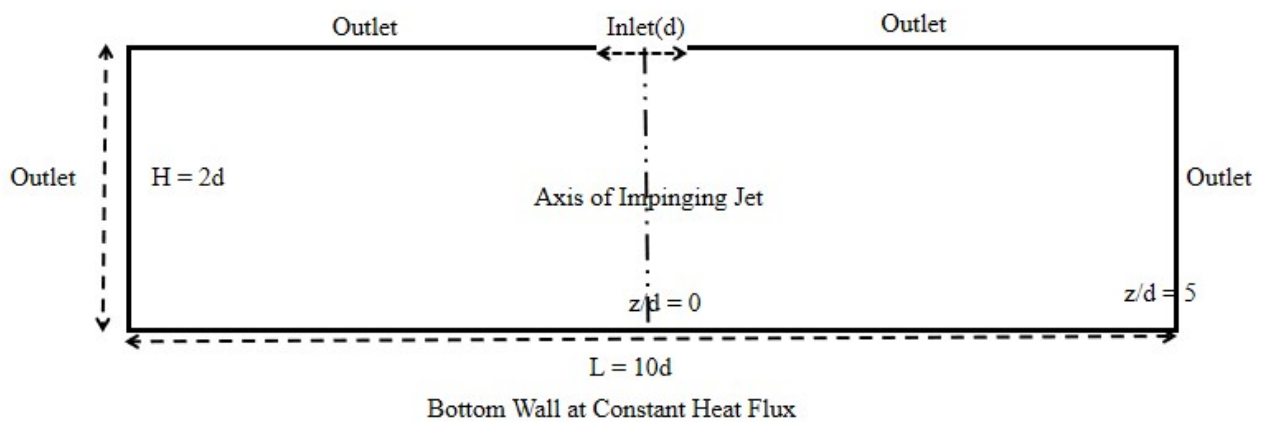


Figure 3.1(a): Sectional view of geometry is illustrated.

Dimensions	Magnitude
d (mm)	20
H/d	2
L/d	10

Table 3.1(a): Geometry illustrated.

Fluid Properties	Values
Density(Kg/m^3)	1.1315
Thermal Conductivity($\text{W}/\text{m K}$)	0.0272
Dynamic Viscosity($\text{Pa}\cdot\text{s}$)	0.000019
Specific Heat ($\text{J}/\text{Kg K}$)	1007.43

Table 3.1(b): Fluid properties

3.2 Methodology:

The mesh should be fine therefore Y^+ is correctly checked such that it can capture the fluid flow near the heated wall which is at constant heat. The first layer of thickness (ΔY_1) is calculated corresponding to Y^+ and then a fine meshing can be generated by giving the first layer of thickness, maximum layers and growth rate of inflation. The mesh details are shown in table 3.2 (a). The total number of nodes and elements in the mesh are 52, 220 and 1, 16,070 respectively. The applied boundary conditions to run the simulation is therefore listed in table 3.2 (b).

Mesh Details	Values
Mesh Type	HEX
Element size(mm)	2
ΔY_1 (mm)	0.2
Growth Rate	1.2
Maximum Layers	10

Table 3.2 (a): Mesh details are illustrated.

Boundary Conditions	Data
Inlet velocity(m/s)	19.31065
Inlet Temperature(K)	311.6
Wall flux($W/m^2 K$)	12,000
Outlet	$P_{gauge} = 0$

Table 3.2(b): Boundary conditions are illustrated

Calculation for Y^+ :

- If $Y^+ < 1$, the first grid cell is located within the laminar sub-layer.
- If $Y^+ > 30$, the first grid cell is located within the viscous sub-layer.
- If $1 < Y^+ < 30$, the first grid cell is located within the viscous sub-layer but not too close to the surface wall.

Firstly, we should calculate the Reynolds number for our model based on the characteristic scales of our geometry such that:

$$Re = \frac{\rho u d}{\mu}$$

where ρ and μ are the fluid density and viscosity respectively, U is the free stream velocity, and d is the pipe diameter.

The definition of the Y^+ value is such that:

$$Y^+ = \frac{\rho u \Delta Y_1}{\mu}$$

The target Y^+ value and fluid properties are known a priori, so we need to calculate the frictional velocity, u , which is defined as:

$$u = \sqrt{\frac{\tau_w}{\rho}}$$

The wall shear stress, τ_w can be calculated from skin friction coefficient, C_f , such that:

$$\tau_w = \frac{1}{2} C_f \rho u^2$$

The ambiguity in calculating ΔY_1 surrounds the value for C_f . Empirical results have been used to provide an estimate to this value:

For External flows: $C_f = 0.058 Re^{-0.2}$

Taking $Y^+ = 7.5$,

$u = 19.31065$ m/s, $d = 0.02$ m, $\rho = 1.1315$ Kg/m³ and $\mu = 0.000019$ Pa-s

$\Delta Y_1 = 0.2$ mm

The boundary condition showing fluent Image for the geometry is shown in figure 3.3(a) below.

Calculation for Inlet Velocity:

$$Re = \frac{\rho u d}{\mu}$$

$$23,000 = \frac{1.1315 \times u \times 0.02}{0.000019}$$

$$u = 19.31065 \text{ m/s}$$

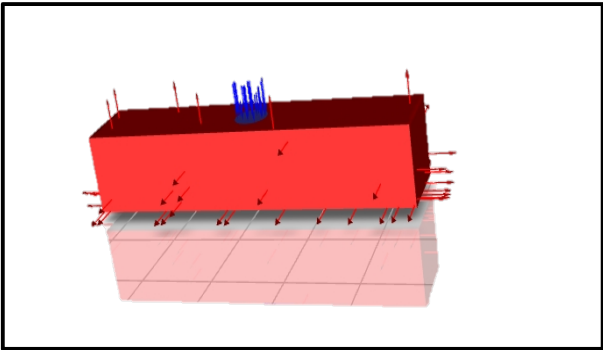


Figure 3.2(a): Showing boundary conditions and flow domain.

The simulation use the SST K Ω model. The simulation is executed for 2000 iterations, and the convergence chart obtained at the 2000th iteration is displayed in table 3.2(c). The simulation employs the SIMPLEC methodology.

Iterations	2000
continuity	5.5618e-04
x-velocity	2.1883e-06
y-velocity	2.6855e-06
z-velocity	2.2922e-06
energy	1.2599e-06
k	1.1722e-05
omega	2.9752e-04

Table 3.2 (c): Convergence chart

3.3 Results and Discussions:

The bottom plate view is shown in figure 3.3(a).

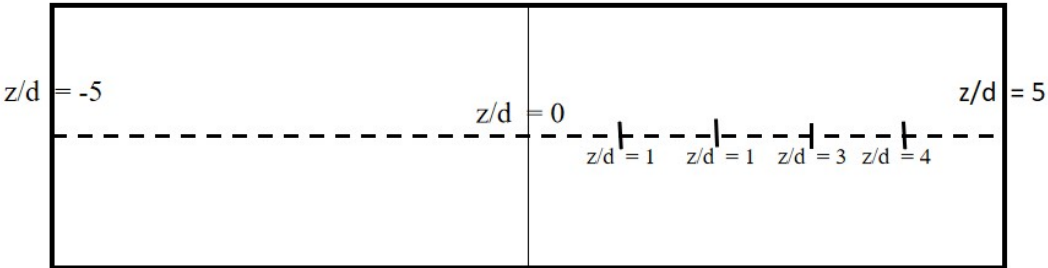


Figure 3.3(a): Bottom plate showing extent of z/d = -5 to z/d = 5, L/d =10

The pressure coefficient on the axis of wall is plotted in Figure 3.3(b) which is along z-zaxis of the geometry. To calculate the pressure coefficient equation 3.3(a) is used. The P is the wall pressure which is first calculated along the axis.

$$C_P = \frac{P-P_{ref}}{\frac{1}{2} \rho V_{Nozzle}^2} \tag{3.3(a)}$$

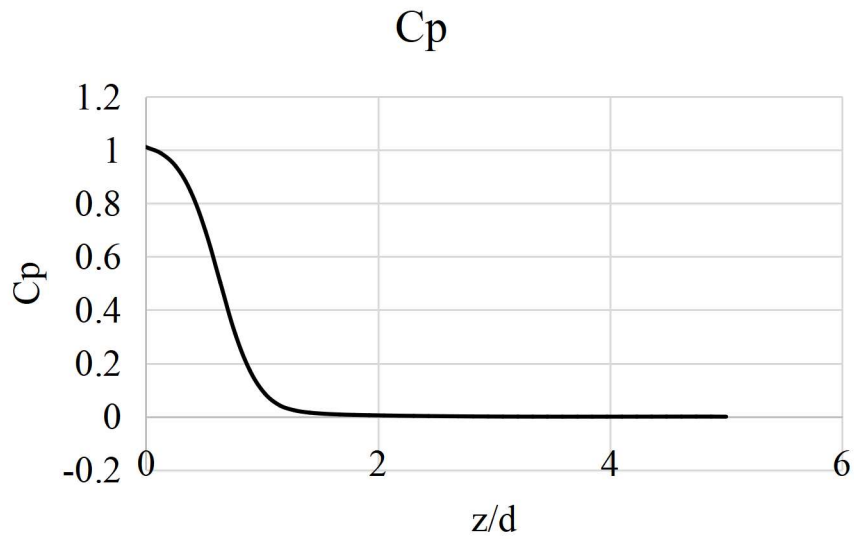


Figure 3.3(b) C_p variation along z/d

Sample Calculation for C_p :

At $z/d = 0.5$

$P = 147 \text{ Pa}$

$P_{ref} = 0$

$$C_p = \frac{P - P_{ref}}{\frac{1}{2} \rho V_{Nozzle}^2}$$

$$= \frac{147 - 0}{\frac{1}{2} \times 1.1315 \times 19.31065^2}$$

$$= 0.697$$

The wall temperature plot along the z -axis is an important aspect in order to predict the heat transfer along the axis. Therefore wall temperature is plotted against the axis z in Figure 3.3 (c). The $z/d = 0$ is the centre-point of the heated wall plate.

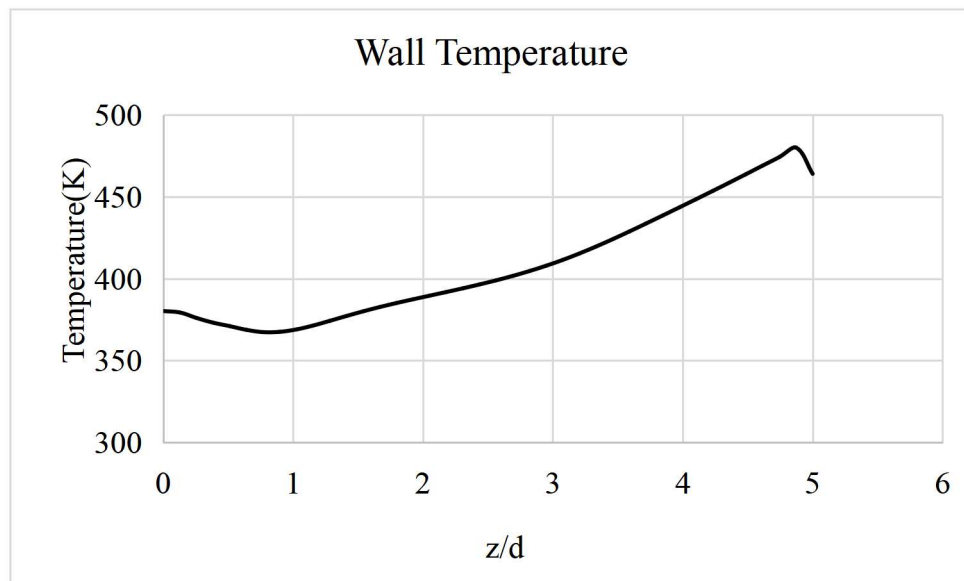


Figure 3.3(c): Wall temperature varying along the axis z/d

The Nu variation is calculated using equation 3.3(b) and 3.3(c) given below.

$$Nu = \frac{h d}{k} \quad 3.3(b)$$

$$h = \frac{q''}{T_w - T_{inlet}} \quad 3.3(c)$$

The obtained Nu variation is plotted in Figure 3.3 (d) below along with Kannan's simulation result. The plot is not exactly superposing each other since some data were missing in his paper. Suitable scheme, models and meshing has been chosen to numerically simulate the problem statement.

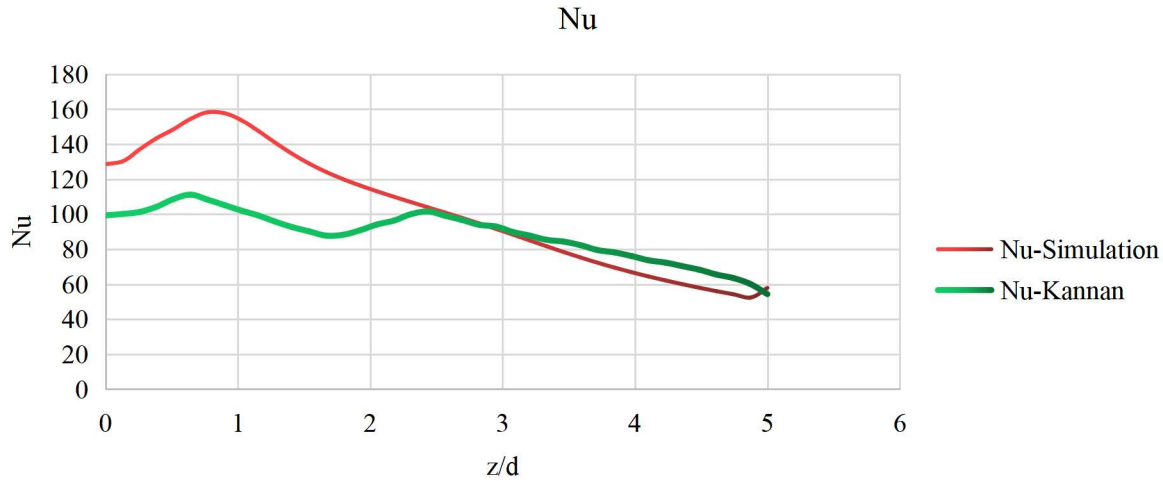


Figure 3.3(d): Nu variation along z/d

Sample Calculation for Nu:

At $z/d = 1$

$T_{wall} = 369 \text{ K}$ and $T_{inlet} = 311.6 \text{ K}$, $q'' = 12000 \text{ W/m}^2$

$$h = \frac{12000}{369 - 311.6} = 209 \text{ W/m}^2\text{K}$$

$$Nu = \frac{209 \times 0.02}{0.0272} = 154$$

4- Numerical Simulation of Steady State Jet Impingement on Flat Plate through cubical plenum.

4.1- Introduction:

A numerical simulation is conducted to study the impact of a jet on a flat plate with a constant heat flux as shown in figure 4.1(a). The geometry used in the simulation includes a nozzle with a diameter of 20mm. The wall plate at the bottom has dimensions of 8d by 8d. The spacing between nozzle exit and wall plate is H which is 3d. The lower plenum plate is entirely solid and features a central nozzle. The bottom plenum has a thickness equal to half of the diameter (d). The dimensions of the cubical plenum above the lower plenum are 4d x 4d x 4d. Thus, the height at which a uniform velocity profile exists can be determined by applying mass conservation principles at the top of the cubical plenum and nozzle, considering that the same fluid enters through the nozzle. The value of Re is assumed to be 23,000. Thus, the nozzle velocity or entrance velocity can be readily calculated using the Reynolds number (Re). The geometric dimensions can be found in table 4.1(a). The fluid properties are similar to what discussed in section 3.

Geometry	Dimensions
d(mm)	20
L/d	8

H/d	3
Nozzle plate	4d x 4d x 0.5d
Cubical Plenum	4d x 4d x 4d

Table 4.1(a): Geometry is illustrated.

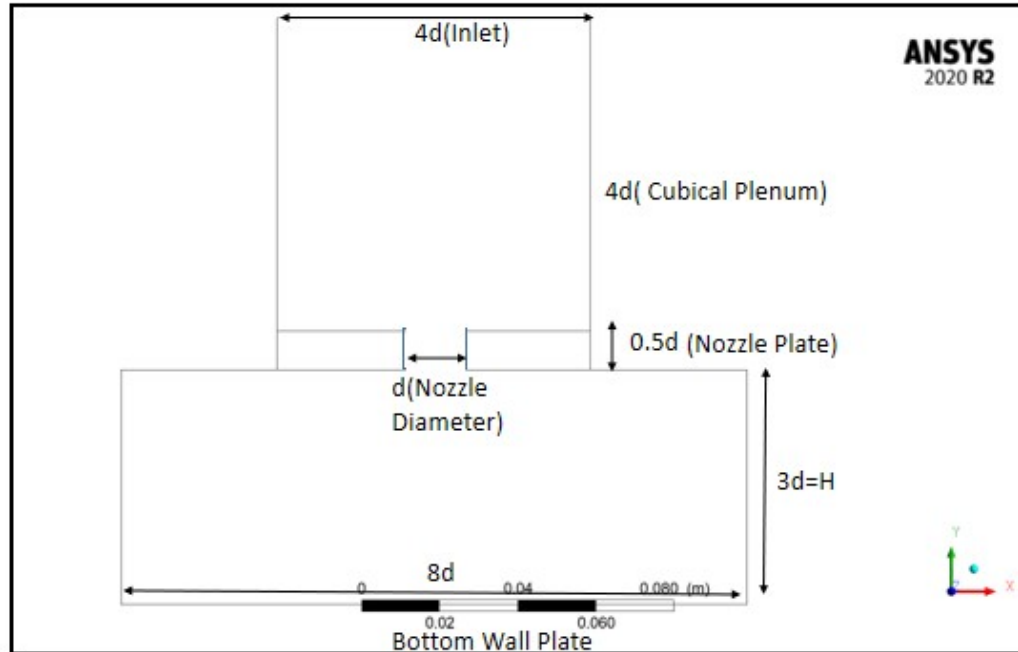


Figure 4.1(a): Sectional view of the cubical plenum geometry is shown with nozzle diameter, $d = 20\text{mm}$, length of bottom plate is $8d$ with width of $8d$. nozzle plate dimension is $4d \times 4d$ with thickness $0.5d$ and cubical plenum height of $4d$ with base on nozzle plate.

4.2- Methodology:

The mesh specifications for the geometry can be found in Table 4.2(a). The grid is positioned adjacent to the wall to precisely and accurately capture the thermal and fluid parameters. The total number of nodes and elements in the mesh are 3, 34,204 and 6, 13,222 respectively. The boundary criteria for the geometry are specified in table 4.2(b), while Figure 4.2(a) displays the flow domain with color-coded markings reflecting the various boundary conditions.

Mesh Details	Values
Mesh Type	HEX
Element size(mm)	2
$\Delta Y1(\text{mm})$	0.2
Growth Rate	1.2
Maximum Layers	10

Table 4.2(a): Mesh details are illustrated

Boundary Conditions	Data
Inlet velocity(m/s)	0.948
Inlet Temperature(K)	311.6
Wall flux($\text{W}/\text{m}^2\text{K}$)	12,000
Outlet	$P_{\text{gauge}} = 0$

Table 4.2(b): Boundary conditions for the geometry.

Calculation for Y^+ :

The Y^+ and $\Delta Y1$ is same since the fluid properties are same and the nozzle entrance velocity is still 19.31065m/s corresponding to $\text{Re} = 23,000$.

Calculation for Inlet velocity:

By applying mass conservation: $\dot{m}_{inlet} = \dot{m}_{nozzle(entrance)}$

Assuming density of fluid remains same at both regions.

$$A_{inlet} u_{inlet} = A_{nozzle} u_{nozzle(entrance)}$$

$$u_{inlet} = \frac{A_{nozzle} u_{nozzle(entrance)}}{A_{inlet}}$$

$$= 0.948 \text{ m/s}$$

The Figure 4.2(a) showing arrow at the top of cubical plenum is at uniform velocity of 0.948m/s. The uniform velocity consideration is however justified in experimental set-up where a uniform velocity of jet is observed at 4d height from the nozzle plate.

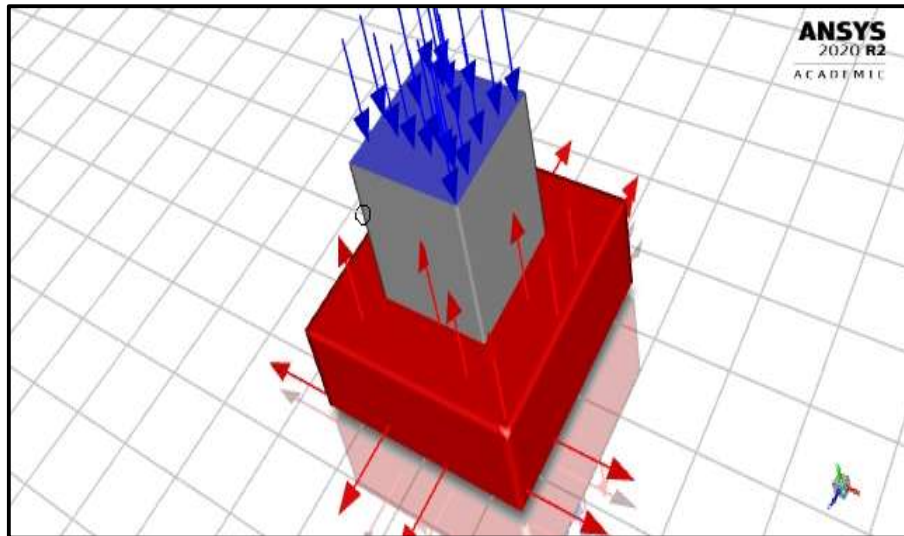


Figure 4.2(a): Marking the boundary conditions and the flow domain.

The simulation use the SST K Ω model. The scheme used is coupled. The simulation is run for 1000 iteration and the observed convergence chart at 1000th iteration is given in table 4.2(c).

Iterations	1000
continuity	5.9035e-04
x-velocity	2.6356e-06
y-velocity	1.2955e-06
z-velocity	2.5947e-06
energy	9.6015e-09
k	2.9780e-06
omega	3.0732e-05

Table 4.2(c): Convergence chart

4.3-Results and Discussion:

The figure 4.3(a) showing bottom plate geometrical dimensions mentioning the extent of distance from center-most point of the impinging plate to the two orthogonal axis x and z. The x-axis is extended from $x/d = 0$ to $x/d = 8$ and the z-axis is extended from $z/d = 0$ to $z/d = 8$.

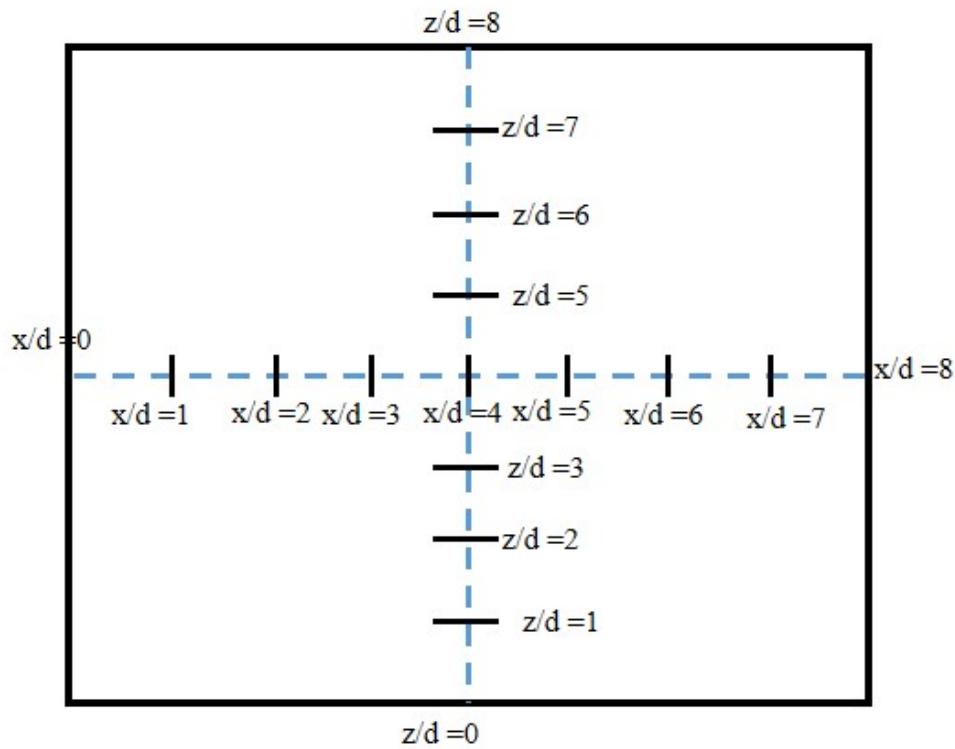


Figure 4.3(a): Figure illustrates the extent of bottom plate along the two orthogonal axis.

The pressure coefficient is graphed along both the orthogonal x and z axes. The pressure coefficient reaches its maximum value when $z/d = 4$, which corresponds to the middle of the plate where the jet impinges directly. The pressure coefficient reaches value of 1.85 along the x-axis at $x/d = 4$ as shown in figure 4.3(b), and a value of 1.87 along the z-axis in figure 4.3(c) at $z/d = 4$.

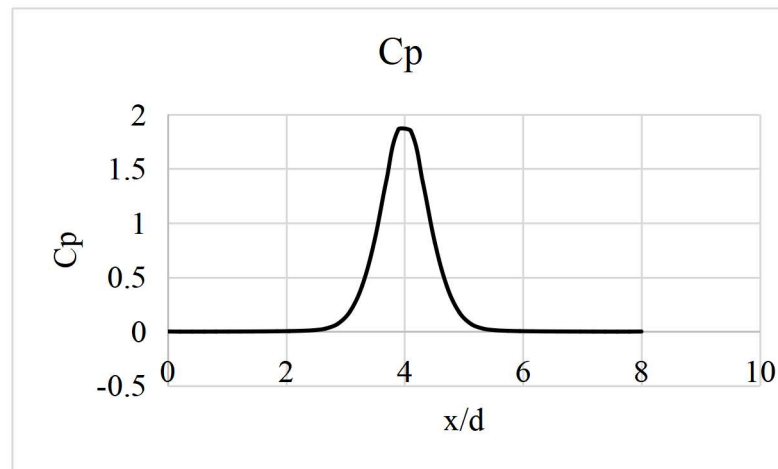


Figure 4.3(b) C_p variation along x/d

Sample calculation for C_p variation along x/d :

At $x/d = 4.15$,

$P = 172$ Pa and $P_{ref} = 0$

$u = 19.31065$ m/s [Nozzle entrance velocity]

$$C_p = \frac{P - P_{ref}}{\frac{1}{2} \rho V_{Nozzle}^2}$$

$$= \frac{172 - 0}{\frac{1}{2} \times 1.1315 \times 19.31065^2} = 0.814$$

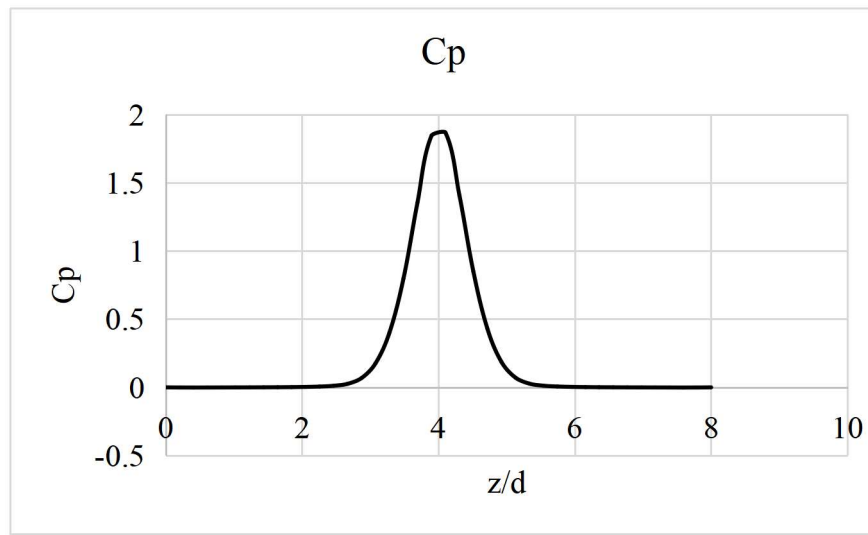


Figure 4.3(c) C_p variation along z/d

Sample Calculation for variation of C_p along z/d :

At $z/d = 4$,

$P = 394$ Pa and $P_{ref} = 0$

$u = 19.31065$ m/s [Nozzle entrance velocity]

$$C_p = \frac{P - P_{ref}}{\frac{1}{2} \rho V_{Nozzle}^2}$$

$$= \frac{394 - 0}{\frac{1}{2} \times 1.1315 \times 19.31065^2} = 1.87$$

The temperature of the wall is graphed along both the x-axis and y-axis in figures 4.3(d) and 4.3(e) below. The wall temperature is utilized to compute the variation of the Nu number along both the axis. Thus, the plot for Nu is also graphed on the x-axis and z-axis in figures 4.3(f) and 4.3(g) accordingly.

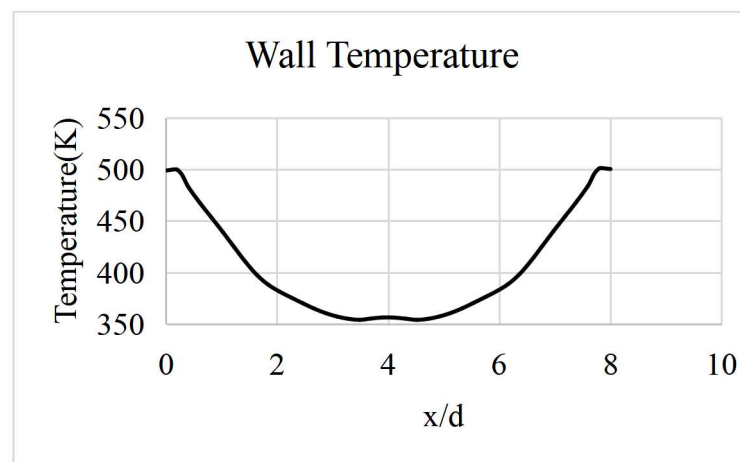


Figure 4.3(d): Wall temperature along x/d

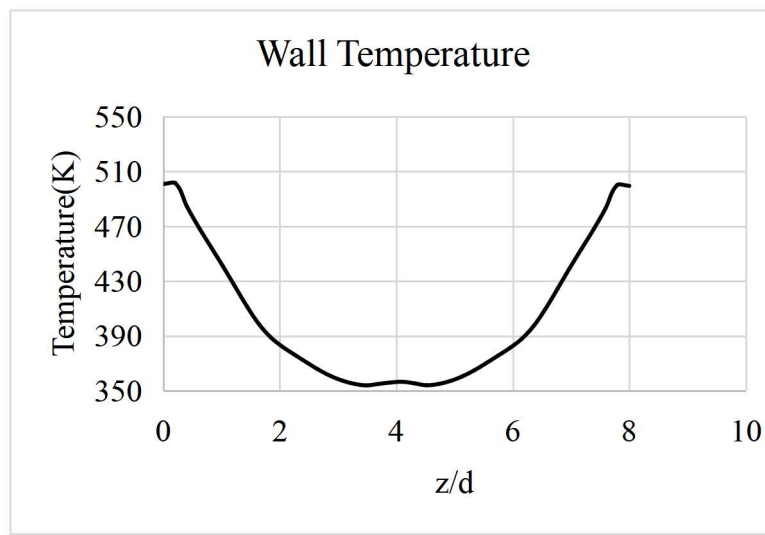


Figure 4.3(e): Wall temperature along z/d

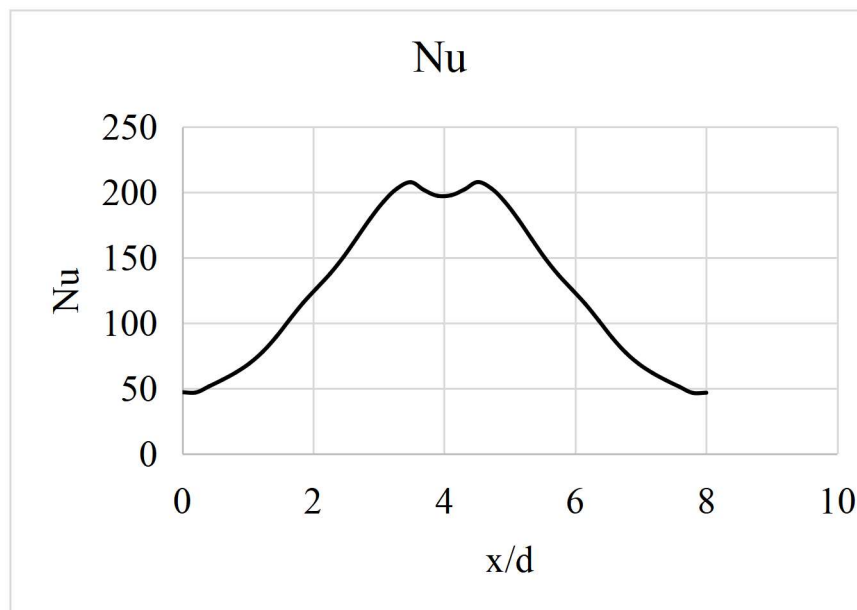


Figure 4.3(f): Nu plot along x/d

Sample Calculation for Nu along x/d :

At $x/d = 6.15$

$T_{wall} = 389 \text{ K}$ and $T_{inlet} = 311.6 \text{ K}$, $q'' = 12000 \text{ W/m}^2$

$$h = \frac{12000}{389 - 311.6} = 156 \text{ W/m}^2\text{K}$$

$$\text{Nu} = \frac{269 \times 0.02}{0.0272} = 115$$

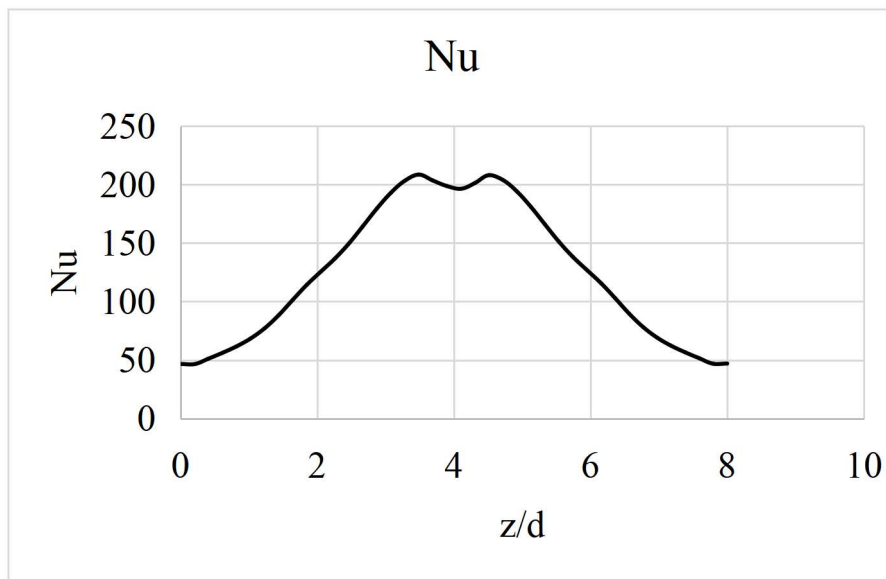


Figure 4.3(g): Nu plot along z/d

Sample Calculation for Nu along z/d :

At $z/d = 4$

$T_{wall} = 357 \text{ K}$ and $T_{inlet} = 311.6 \text{ K}$, $q'' = 12000 \text{ W/m}^2$

$$h = \frac{12000}{357 - 311.6} = 267 \text{ W/m}^2\text{K}$$

$$Nu = \frac{267 \times 0.02}{0.0272} = 197$$

Figure 4.3(h) presents a comprehensive diagram illustrating the streamline throughout the whole flow domain. The uppermost area represents the domain with a consistent inflow velocity, which serves as the starting point for the entire simulation. The area where streamlines converge is known as the aperture or nozzle, through which the jet enters the domain. The absence of slip conditions along the walls and periphery of the nozzle is attributed to the lower plenum or nozzle plate. The wire-frame is extended from 0 to $8d$, with $8d$ representing the total length of the impinging plate.

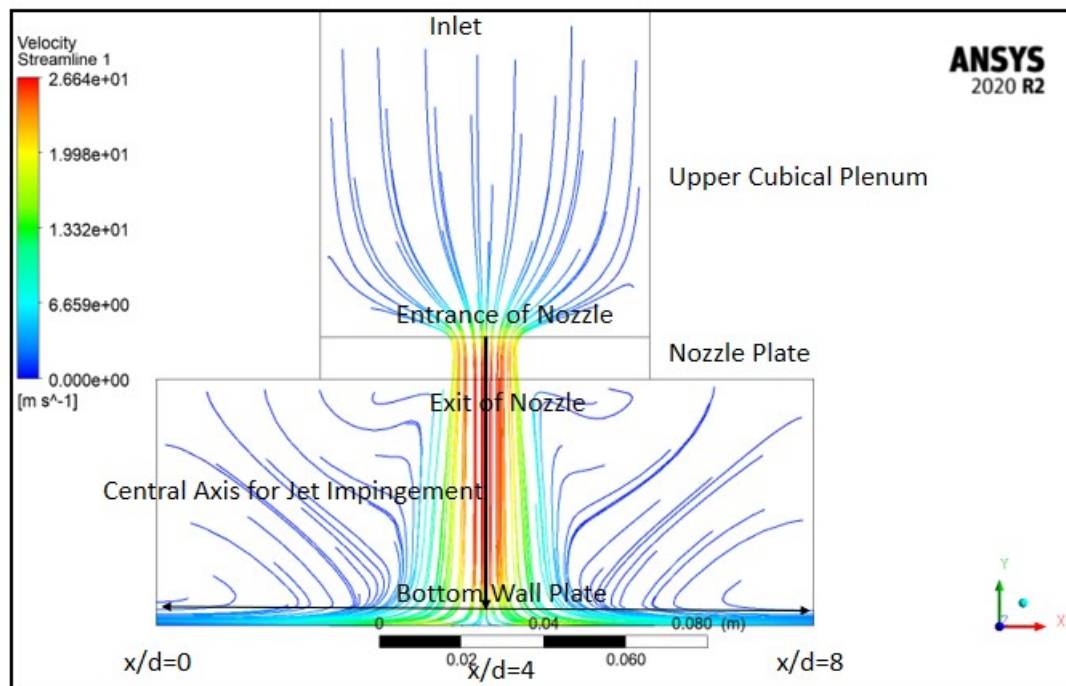


Figure 4.3(h) illustrates the centre plane over which the streamlines are depicted with $H/d = 3$

It is crucial to consider the flow of velocity vectors when evaluating the variation in the pressure coefficient at the heated wall, particularly by observing the vectors near the orifice. Consequently, Figure 4.3(i) schematically illustrates the velocity vectors in proximity to the nozzle.

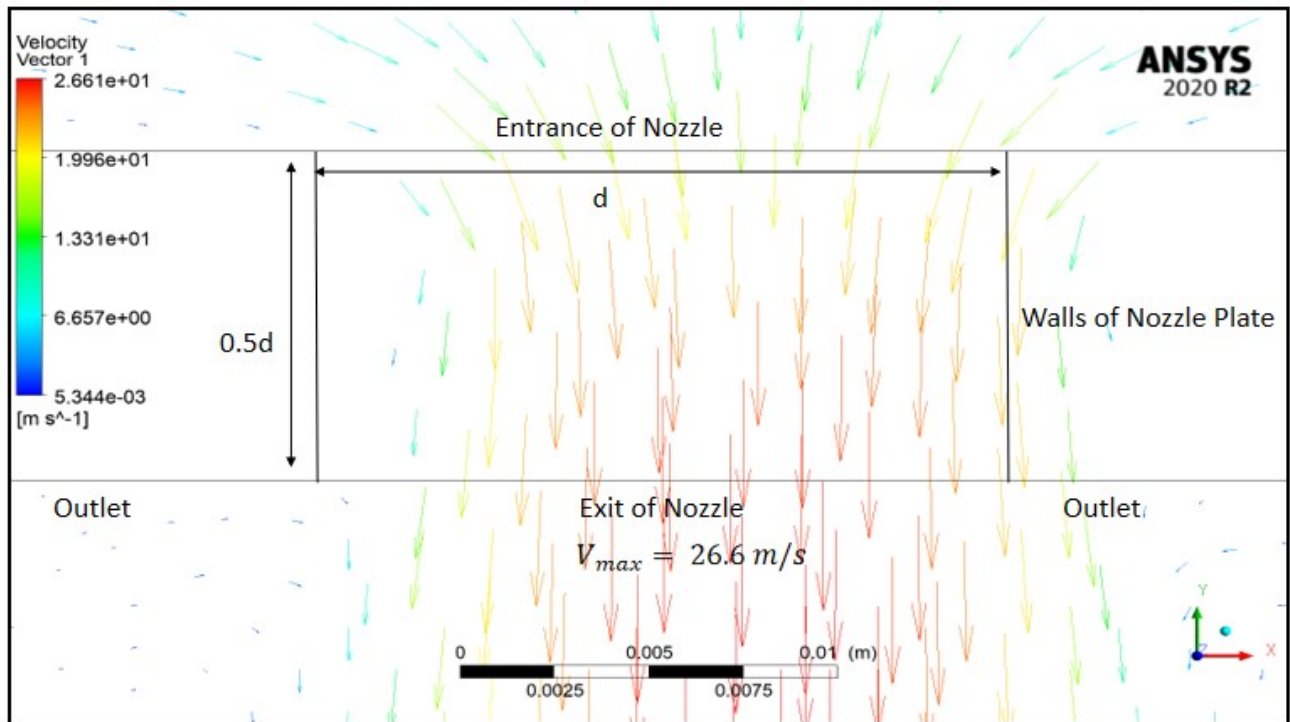


Figure 4.3(i): Showing velocity vectors near the nozzle. Entrance nozzle velocity is 19.31065 m/s and maximum velocity is 26.6 m/s. Nozzle plate thickness $0.5d$

Figure 4.3(j) illustrates the velocity vectors in close proximity to the bottom heated wall. The velocity at the wall is zero as a result of the no slip condition, as illustrated in the figure. The plot is marked from $x/d = 4$ to $x/d = 8$.

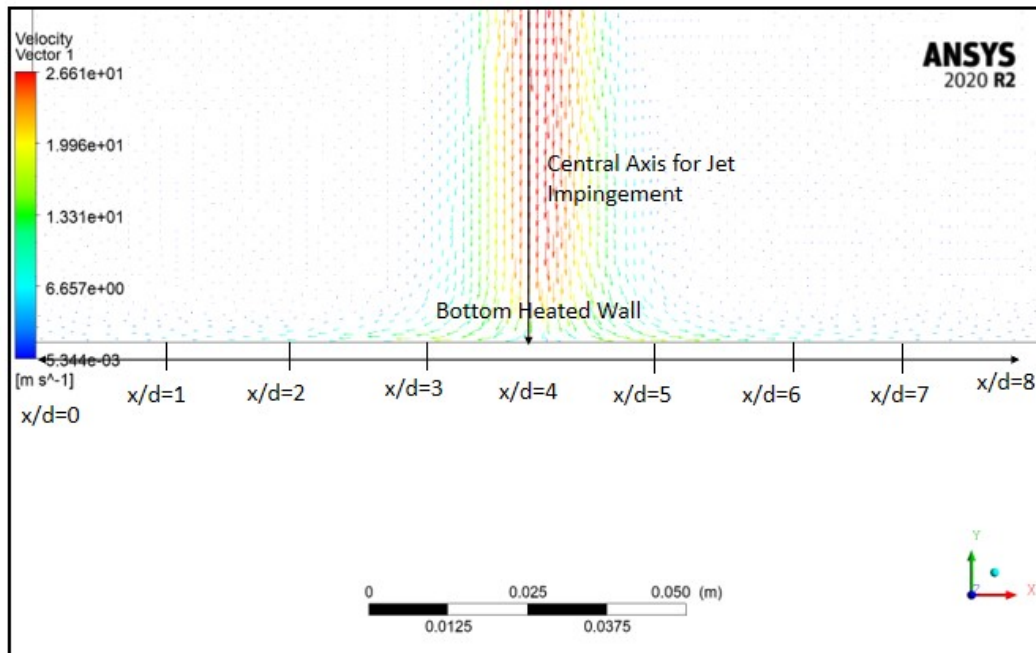


Figure 4.3(j): Velocity vectors close to the wall

5- Numerical Simulation of Steady State Jet Impingement on Flat Plate through concave plenum

5.1- Introduction:

The geometry utilized for simulation in section 4 has been altered as shown in figure 5.1(a). Now, the concave plenum has supplanted the top cubical plenum. The purpose of this procedure is to observe various flow patterns and comprehend the heat transfer operation on the wall plate under varying geometric conditions. The sole modification to the geometry in section 4 of this report is that the concave plenum has been modified to have a concave diameter of (D) 48mm and a wall thickness of 5 mm for the upper plenum. In this instance, the upper plenum is 4d in height and the lower plenum is 0.5d in thickness. In the lower plenum, the nozzle of the geometry is a central orifice. The dimensions of the geometry are illustrated in Table 5.1(a), while the fluid properties are same as per last plenum configuration discussed in section 4.

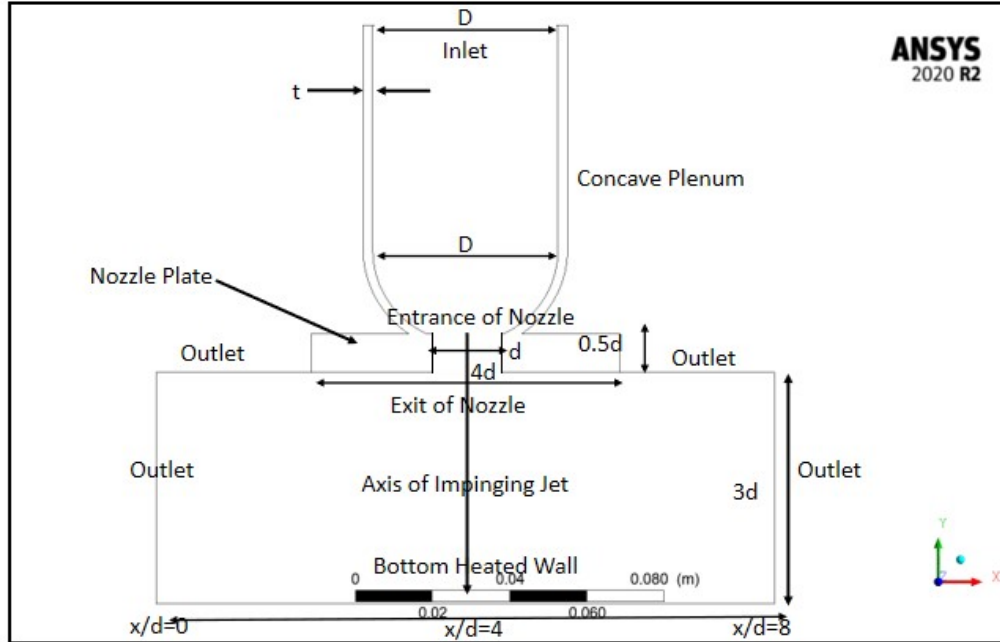


Figure 5.1(a): Sectional view of concave plenum geometry is shown. Nozzle has uniform diameter of d and concave plenum of diameter D with wall thickness ' t '. The nozzle plate thickness $0.5d$. The $H/d = 3$ and bottom wall plate extended with $L = 8d$.

Geometry	Dimensions
d (mm)	20
D (mm)	48
Heated Wall	$8d \times 8d$
H/d	3
Nozzle plate thickness	$0.5d$
Concave plenum height	$4d$
Concave plenum thickness(mm)	5

Table 5.1(a): Geometry is illustrated

5.2-Methodology:

The geometry mesh details are presented in Table 5.2(a). It has a linear element order of 2 mm in dimension. This mesh is tetragonal. The fluid and thermal transfer phenomena are captured by utilizing the inflation layers near the wall to generate boundary layers. The SST-K- Ω model is employed to simulate the circumstance, and the coupled scheme is implemented to optimize convergence. The situation's boundary conditions dictate that the nozzle velocity at the entrance is 19.31065 m/s, which corresponds to Re 23000. The velocity is consistent at the inlet, which is located at the summit of the upper plenum. Mass conservation can be used to establish the boundary condition of uniform velocity at the inlet and nozzle entrance regions, as the same fluid is entering the region.

Meshing Details	Values
Mesh Type	Tetragonal
Element size (mm)	2
First layer thickness(mm)	0.2
Growth Rate	1.2
Maximum layers	10

Boundary Conditions	Data
Inlet velocity(m/s)	1.5798
Inlet Temperature(K)	311.6
Wall flux(W/m ² K)	12000
Outlet	$P_{gauge} = 0$

Table 5.2(a): Grid Details

Table 5.2(b): Boundary Conditions

Calculation for Y^+ :

The Y^+ and ΔY_1 is same since the fluid properties are same and the nozzle entrance velocity is still 19.31065m/s corresponding to $Re = 23,000$.

Figure 5.2(a) illustrates the 3D complete geometry and pictorial representation of the fluid domain. The velocity at the inlet is 1.5798 m/s, as determined by mass conservation, as the nozzle velocity is 19.31065 m/s.

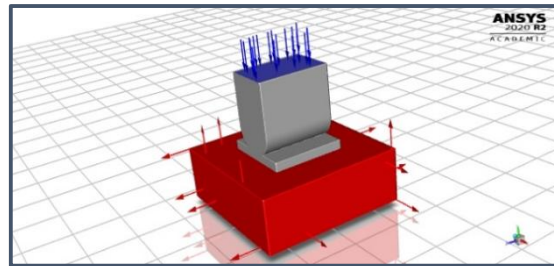


Figure 5.2(a): 3D representation of geometry showing inlet velocity, walls and pressure outlet with arrows.

Calculation of inlet velocity:

By applying mass conservation: $\dot{m}_{inlet} = \dot{m}_{nozzle(entrance)}$

Assuming density of fluid remains same at both regions.

$$A_{inlet} u_{inlet} = A_{nozzle} u_{nozzle(entrance)}$$

$$u_{inlet} = \frac{A_{nozzle} u_{nozzle(entrance)}}{A_{inlet}}$$

$$= 1.5798 \text{ m/s}$$

The convergence chart for running 1000 iterations in mentioned in table 5.2(c).

Iterations	1000
Continuity	2.7460e-08
x-velocity	5.5589e-05
y-velocity	1.4926e-04
z-velocity	7.3152e-05
Energy	3.4779e-08
k	6.6615e-05
omega	2.5908e-04

5.3-Results and Discussions:

The figure 4.3(a) showing bottom plate geometrical dimensions mentioning the extent of distance from center-most point of the impinging plate to the two orthogonal axis x and z. The x-axis is extended from $x/d = 0$ to $x/d = 8$ and the z-axis is extended from $z/d = 0$ to $z/d = 8$.

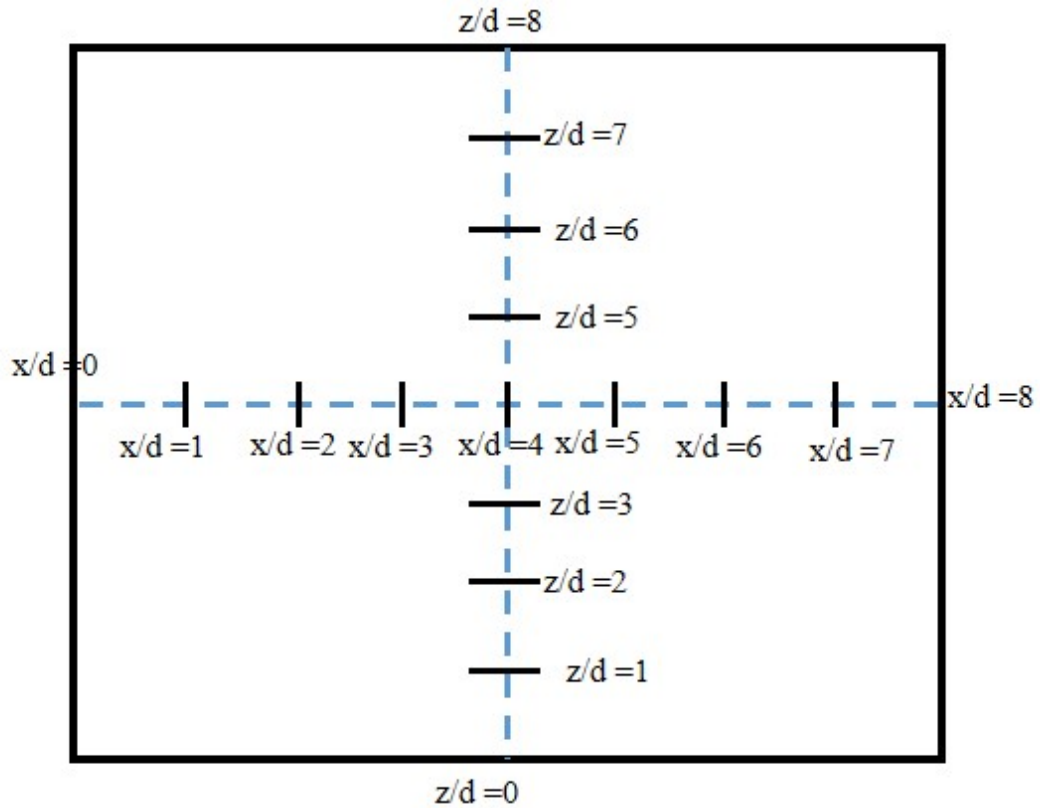


Figure 5.3(a): Bottom plate for concave plenum geometry. Both x and z axis are orthogonal to each other.

The pressure coefficient is a critical parameter for comparing the results of various geometries under the same $H/d = 3$ configuration. Consequently, the wall pressure in the x and z axes of the constant heat flux wall at the bottom can be employed to generate the pressure coefficient diagram. The pressure coefficient at the wall is depicted in Figure 5.3(b) and Figure 5.3(c) at varying locations. The pressure coefficient at $x/d = 4$ is 1.3165 in figure 5.3(b) and 1.33 in figure 5.3(c).

Sample calculation for C_p variation along x/d:

At $x/d = 4$,

$P = 278$ Pa and $P_{ref} = 0$

$u = 19.31065$ m/s [Nozzle entrance velocity]

$$C_p = \frac{P - P_{ref}}{\frac{1}{2} \rho V_{Nozzle}^2}$$

$$= \frac{278 - 0}{\frac{1}{2} \times 1.1315 \times 19.31065^2} = 1.32$$

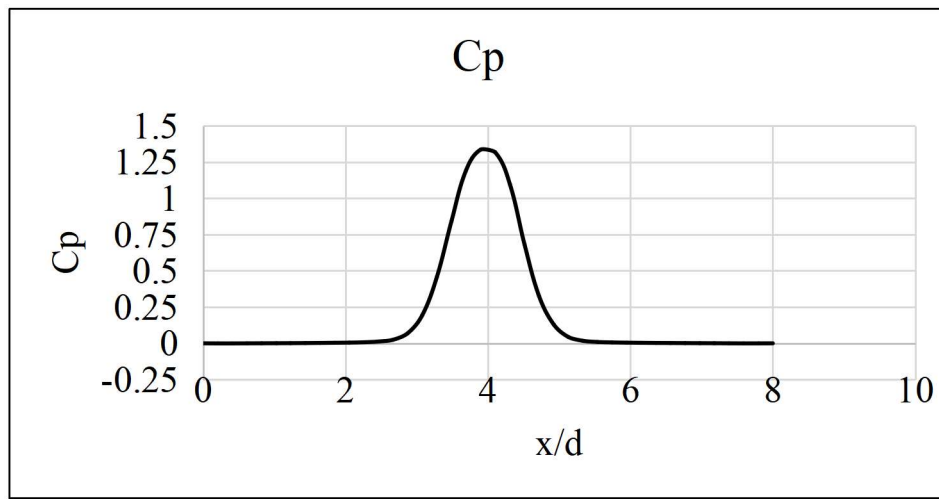


Figure 5.3(b): C_p variation along x/d

Sample Calculation for variation of C_p along z/d :

At $z/d = 4.15$,

$P = 139$ Pa and $P_{ref} = 0$

$u = 19.31065$ m/s [Nozzle entrance velocity]

$$C_p = \frac{P - P_{ref}}{\frac{1}{2} \rho V_{Nozzle}^2}$$

$$= \frac{139 - 0}{\frac{1}{2} \times 1.1315 \times 19.31065^2} = 0.658$$

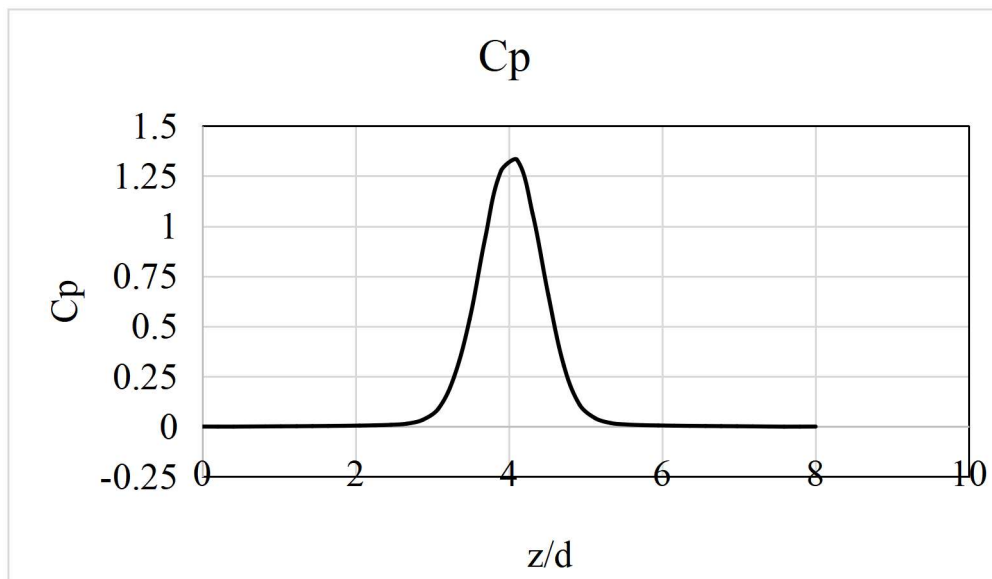


Figure 5.3(c): C_p variation along z/d

The wall temperature is important to calculate the Nu variation therefore the wall temperature is plotted. Figure 5.3(d) and Figure 5.3(e) shows variation of wall temperature along x/d and z/d respectively.

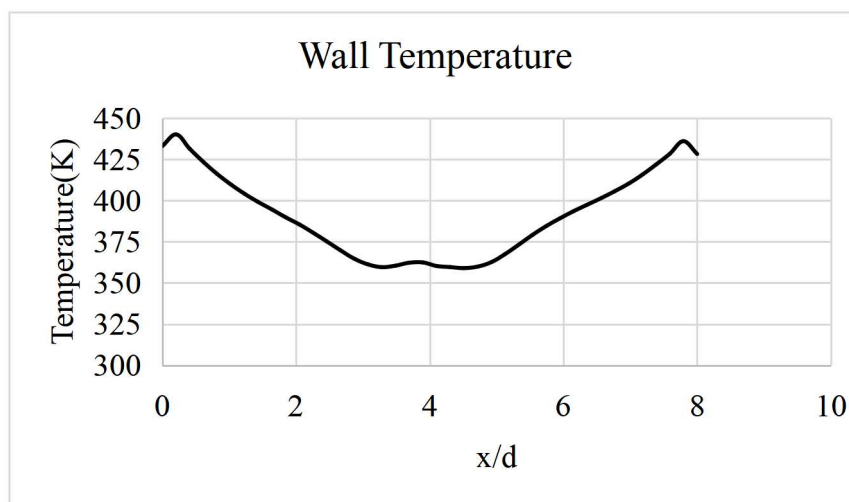


Figure 5.3(d): Wall temperature along x/d

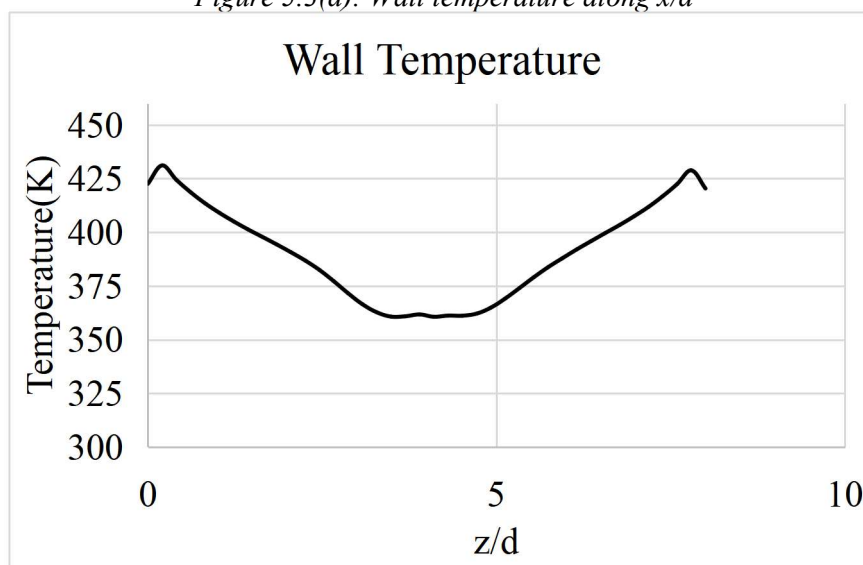


Figure 5.3(e): Wall temperature along z/d

The wall temperature and inlet temperature of the jet can be used to calculate the Nu. The Nu variation plot is depicted in figure 5.3(f) and figure 5.4(g) along the x- and z-axes, respectively.

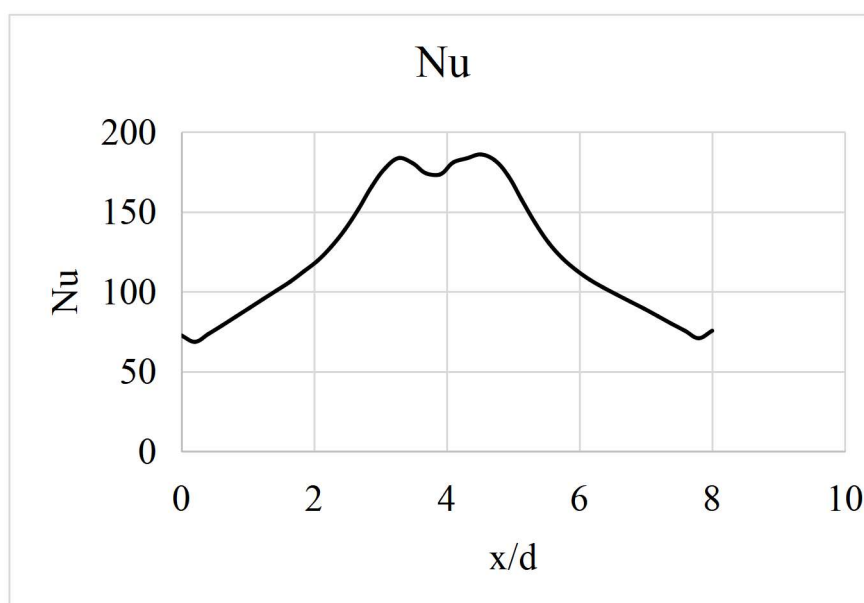


Figure 5.3(f): Nu variation along x/d

Sample Calculation for Nu along x/d:

At $x/d = 4$

$T_{wall} = 360 \text{ K}$ and $T_{inlet} = 311.6 \text{ K}$, $q'' = 12000 \text{ W/m}^2$

$$h = \frac{12000}{360 - 311.6} = 246 \text{ W/m}^2\text{K}$$

$$Nu = \frac{246 \times 0.02}{0.0272} = 181$$

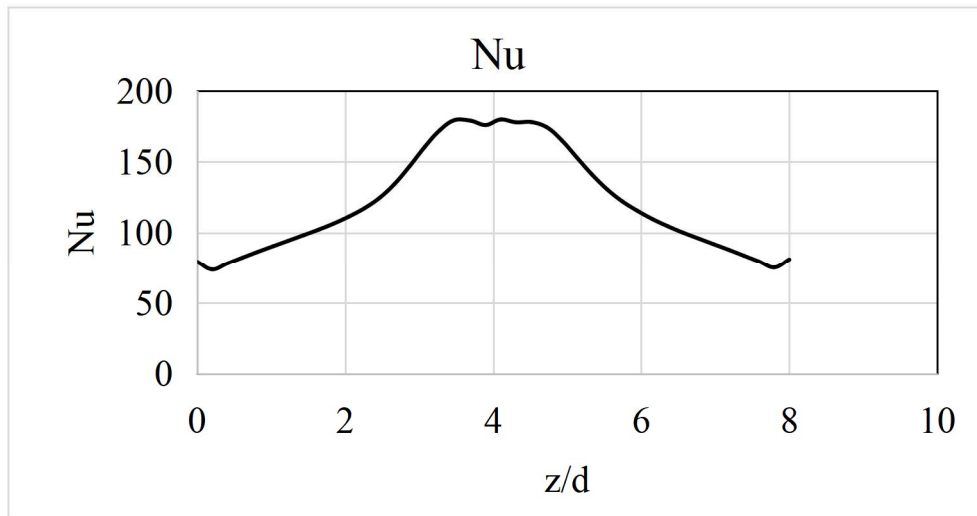


Figure 5.3(g): Nu variation along z/d

Sample Calculation for Nu along z/d:

At $z/d = 6.15$

$T_{wall} = 392 \text{ K}$ and $T_{inlet} = 311.6 \text{ K}$, $q'' = 12000 \text{ W/m}^2$

$$h = \frac{12000}{392 - 311.6} = 149 \text{ W/m}^2\text{K}$$

$$Nu = \frac{245 \times 0.02}{0.0272} = 110$$

The streamline is schematically depicted in figure 5.3(h) from the inlet to the wall plate. The nozzle through which the jet passes is indicated by the convergence of these streamlines at a specific location in the middle of the geometry. The entire length of the plate, denoted by $L = 8d$, is represented by the wire-frame located at the plate's base.

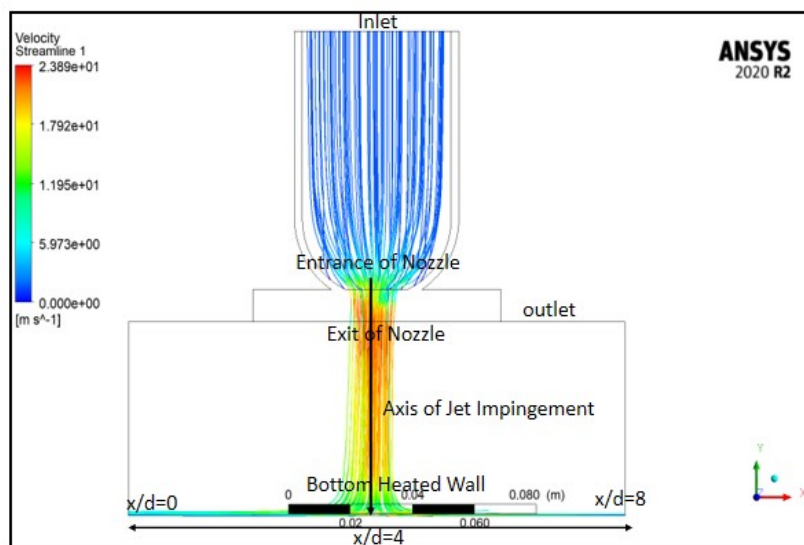


Figure 5.3(h): Streamline is schematically shown with $H/d=3$

The velocity vectors close to the entrance and exit of nozzle is very important to provide an explanation for pressure coefficient variation even with same $H/d=3$. Therefore Figure 5.3(i) shows velocity vectors near the entrance and exit region of the nozzle.

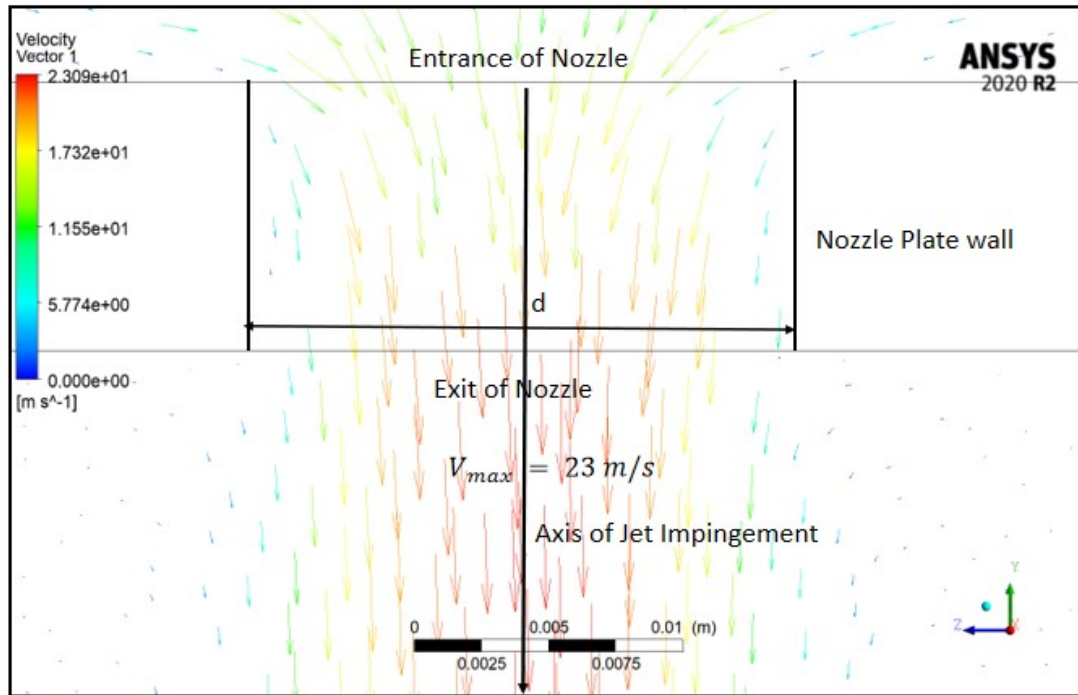


Figure 5.3(i): Velocity vectors near the nozzle. Nozzle diameter (d) and plenum plate thickness is $0.5d$. The maximum velocity is 23 m/s and the entrance nozzle velocity is 19.31065 m/s

Figure 5.3(j) illustrates the velocity vectors in close proximity to the jet impinging plate. The blue colour of the vectors that are in close proximity to the periphery of the heated wall indicates that there is no slip condition.

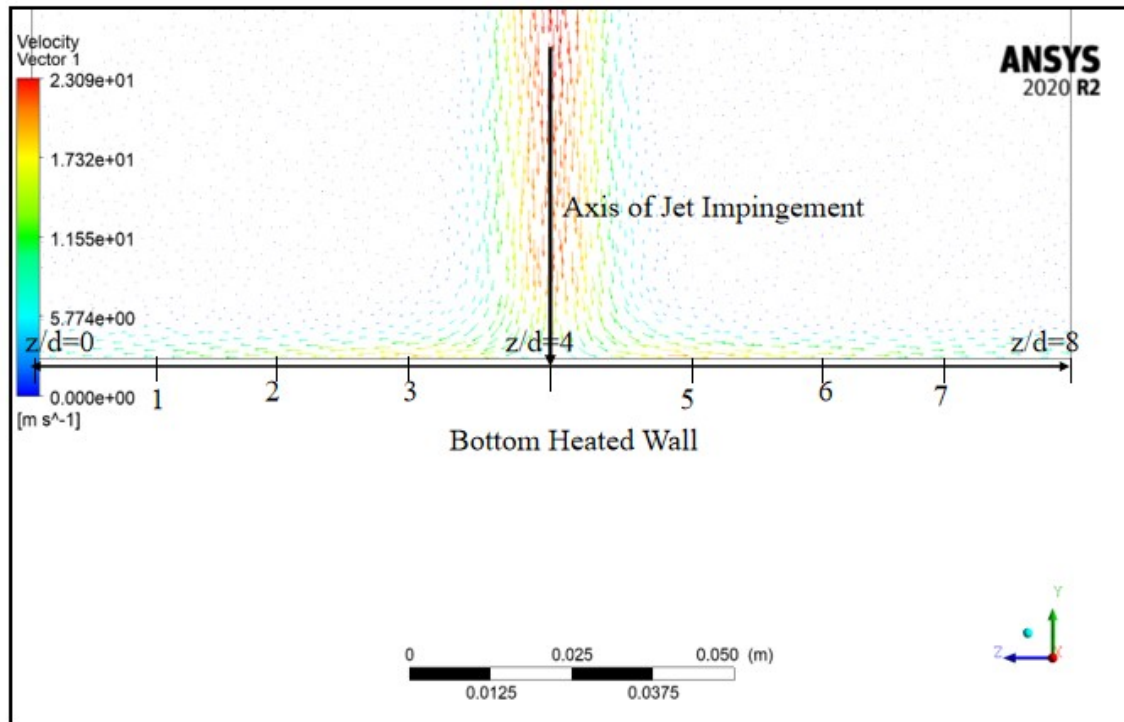


Figure 5.3(j): Vectors close to the heated wall is shown from $x/d=0$ to $x/d=8$

6- Numerical Simulation of Steady State Jet Impingement on Flat Plate through cylindrical plenum

6.1-Introduction:

Simulating the jet impingement on a flat plate through a cylindrical plenum is straightforward. The sole alteration to the geometry is the addition of a cylindrical plenum over the nozzle, at a height of $3d$ and a diameter of the same as shown in figure 6.1(a). The fluid enters through the top face of cylindrical plenum and finally impinges on the flat plate by passing through the nozzle. The geometry is summarized in table 6.1(a), and the fluid properties are same as discussed in section 4 of the report.

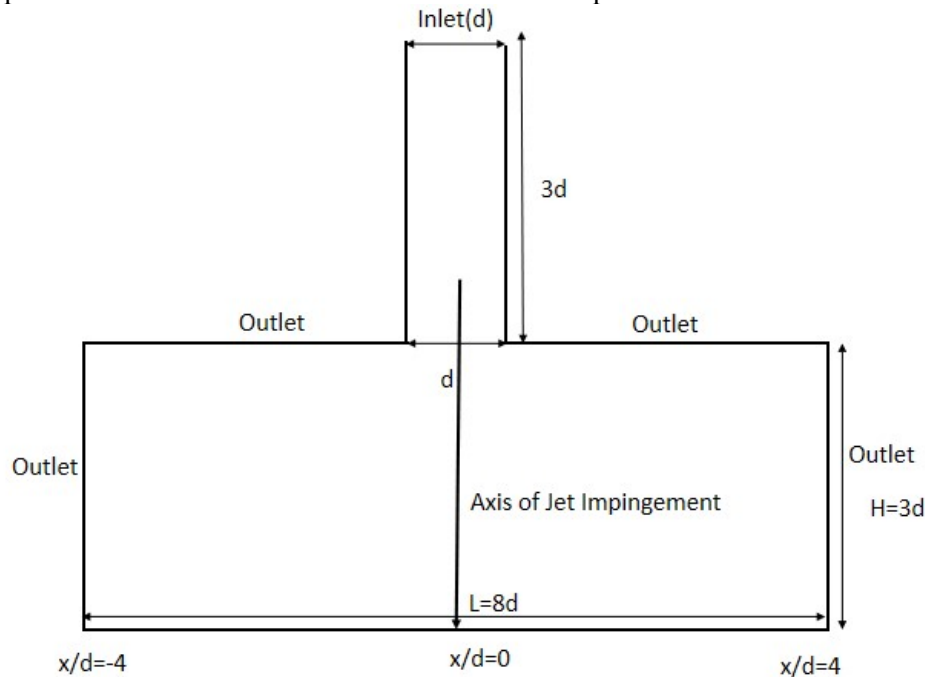


Figure 6.1(a): Sectional view of Geometry is illustrated. Inlet diameter is d , $H = 3d$, $L = 8d$ and Nozzle diameter is d .

Geometry	Dimensions
$d(\text{mm})$	20
H/d	3
L/d	8
Cylindrical plenum Height(mm)	$3d$

Table 6.1(a): Geometry is illustrated

6.2-Methodology:

To accurately calculate the Nu variation along the wall plate in both orthogonal directions and capture the flow of fluid, the mesh is fine near the walls. The grid details are summarized in table 6.2(a). The lattice is maintained in quadratic order with an element size of 1.5 mm. The grid is qualitatively hexagonal, which is achieved by employing the multi zone command in Fluent. The total number of nodes and elements in the mesh are 27,67,361 and 9,51,691 respectively.

Mesh Details	Values
Mesh Type	HEX
Element size(mm)	1.5
First layer thickness	0.02
Growth Rate	1.2
Maximum layers	15

Table 6.2(a): Grid Details are mentioned

Boundary Conditions	Data
Inlet velocity(m/s)	1.5798
Inlet Temperature(K)	311.6
Wall flux($\text{W}/\text{m}^2\text{K}$)	12000
Outlet	$P_{\text{gauge}} = 0$

Table 6.2(b): Boundary Conditions

Calculation for Y^+ :

The Y^+ and ΔY_1 is same since the fluid properties are same and the nozzle entrance velocity is still 19.31065m/s corresponding to $Re = 23,000$.

Figure 6.2(a) illustrates the boundary conditions and flow domain in a colorized pictorial representation. The inlet velocity is determined using mass conservation, as the velocity at the nozzle's entrance is 19.31065 m/s, which corresponds to $Re = 23000$.

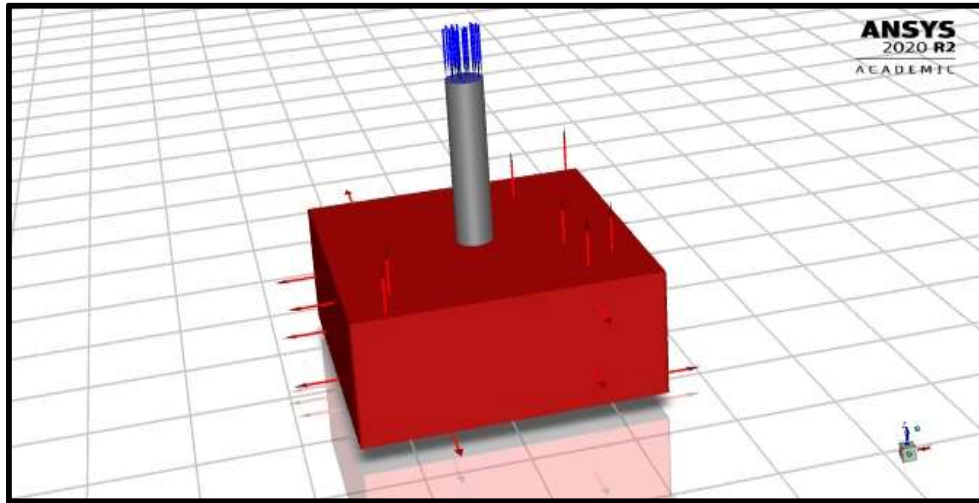


Figure 6.2(a): Flow domain, pressure outlet, plenum and inlet velocity at the top of plenum is mentioned.

Calculation of inlet velocity:

By applying mass conservation: $\dot{m}_{inlet} = \dot{m}_{nozzle(entrance)}$

Assuming density of fluid remains same at both regions.

$$A_{inlet} u_{inlet} = A_{nozzle} u_{nozzle(entrance)}$$

$$u_{inlet} = \frac{A_{nozzle} u_{nozzle(entrance)}}{A_{inlet}}$$

$$= 19.31065 \text{ m/s} = u_{nozzle(entrance)}$$

The simulation with the Coupled scheme is conducted using the SST-K- Ω model. The solution ultimately converged at 415 iterations after the simulation was run for 1000 iterations. The convergence chart at the 415th iteration is presented in table 6.2(c).

Iteration	415
Continuity	2.2743e-04
x-velocity	2.3898e-07
y-velocity	2.4435e-07
z-velocity	1.3454e-07
Energy	7.8698e-09
K	2.7419e-07
omega	2.4051e-07

Table 6.2(c): Convergence chart

6.3-Results and Discussions:

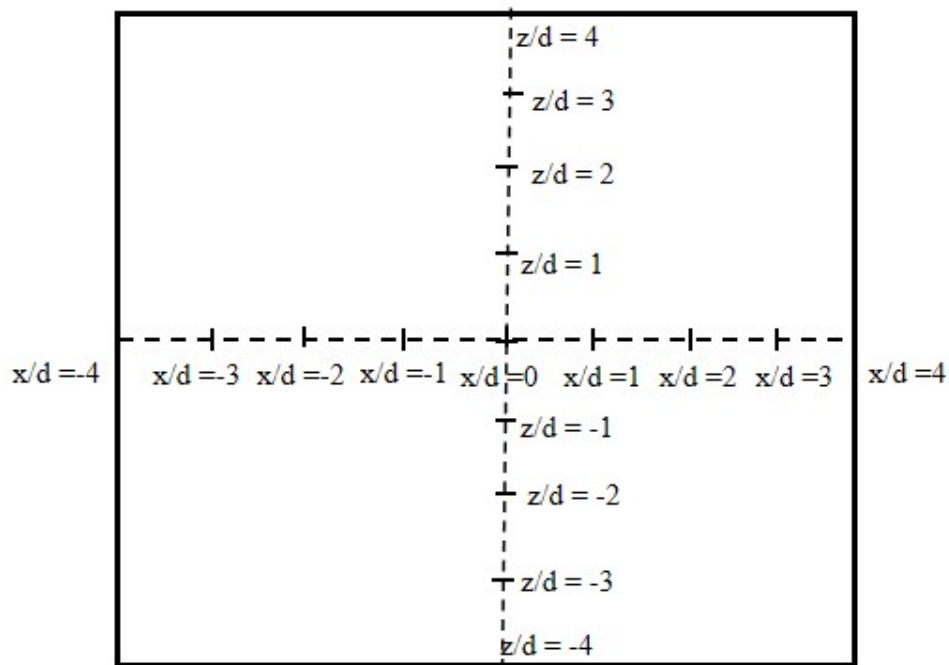


Figure 6.3(a): Bottom plate for concave plenum geometry. Both x and z axis are orthogonal to each other.

The pressure coefficient for cylindrical plenum case is plotted along x and z axis of the wall plate in figure 6.3(b) and 6.3(c).

Sample calculation for C_p variation along x/d :

At $x/d = 0$,

$P = 243 \text{ Pa}$ and $P_{ref} = 0$

$u = 19.31065 \text{ m/s}$ [Nozzle entrance velocity]

$$C_p = \frac{P - P_{ref}}{\frac{1}{2} \rho V_{Nozzle}^2}$$

$$= \frac{243 - 0}{\frac{1}{2} \times 1.1315 \times 19.31065^2} = 1.15$$

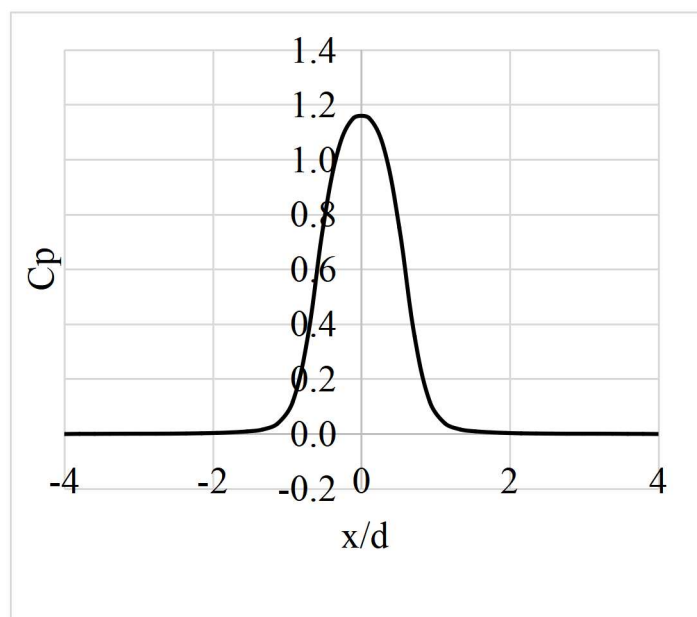


Figure 6.3(b): C_p variation along x/d

Sample Calculation for variation of C_p along z/d :

At $z/d = 0.718$

$P = 75.6 \text{ Pa}$ and $P_{ref} = 0$

$u = 19.31065 \text{ m/s}$ [Nozzle entrance velocity]

$$C_p = \frac{P - P_{ref}}{\frac{1}{2} \rho V_{Nozzle}^2}$$

$$= \frac{75.6 - 0}{\frac{1}{2} \times 1.1315 \times 19.31065^2} = 0.358$$

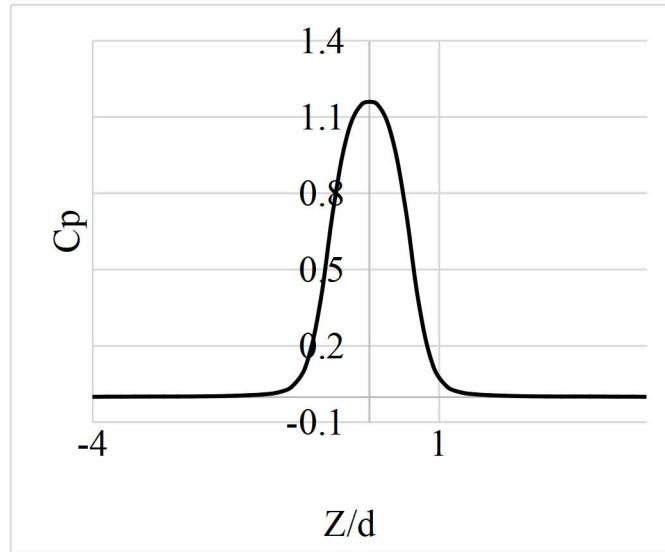


Figure 6.3(c): C_p variation along Z/d

The wall temperature plot is shown again along both the orthogonal axis i.e. along x and z axis in figure 6.3 (d) and 6.3(e).

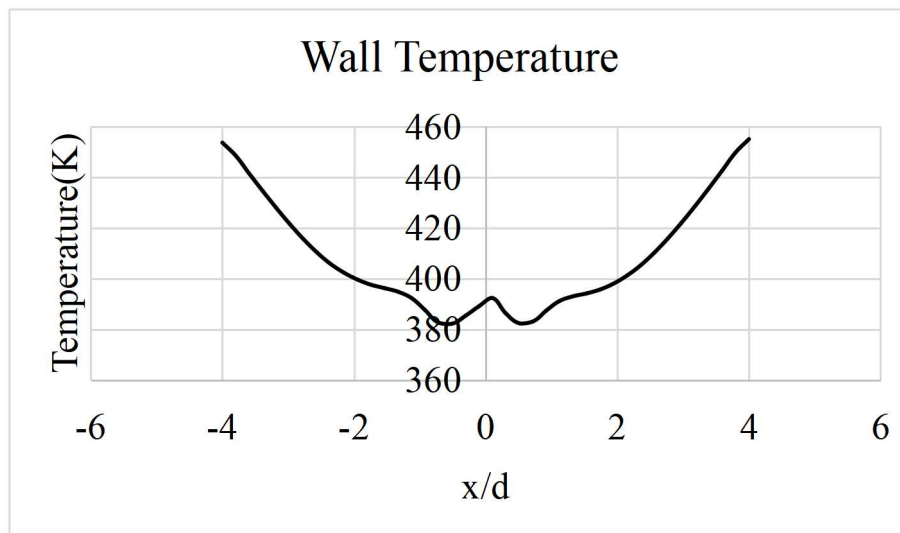


Figure 6.3(d): Wall temperature along x/d

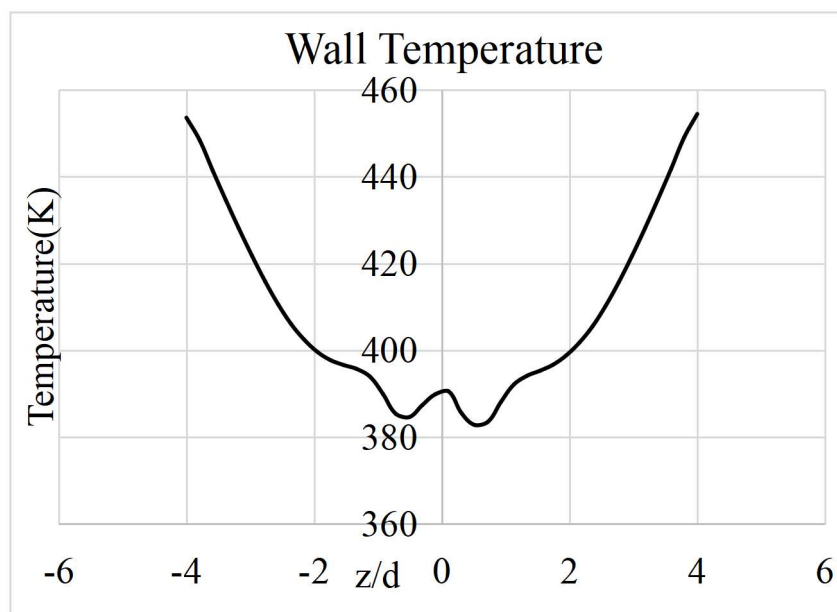


Figure 6.3(e): Wall temperature along z/d

Figures 6.3(f) and 6.3(g) show the Nu estimated from wall and jet inlet temperatures, shown along the x and z axes, respectively.

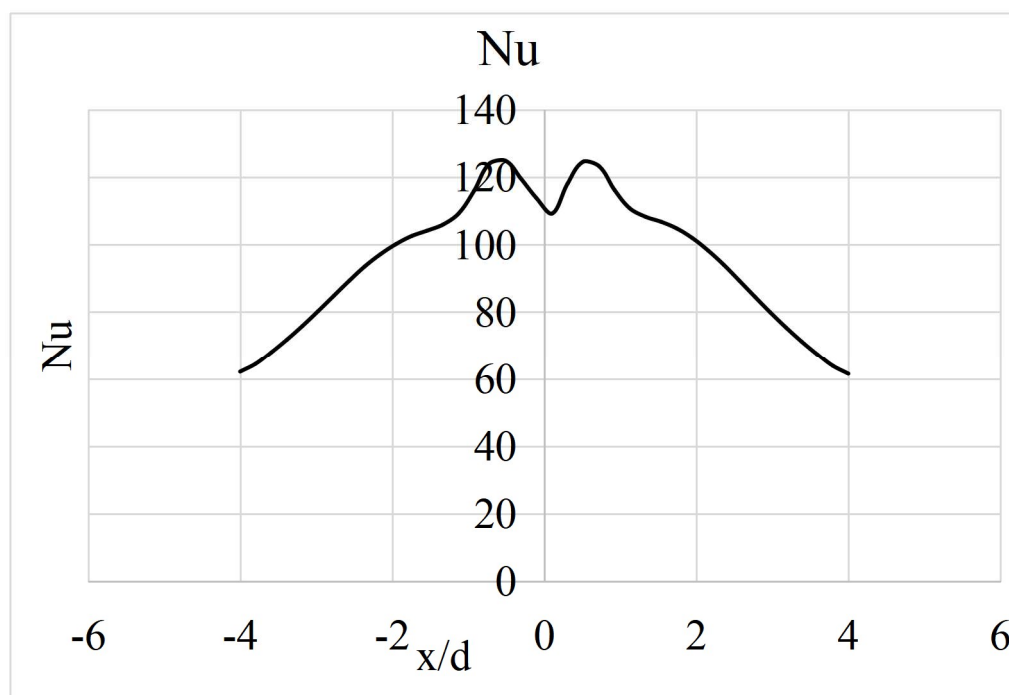


Figure 6.3(f): Nu variation along x/d

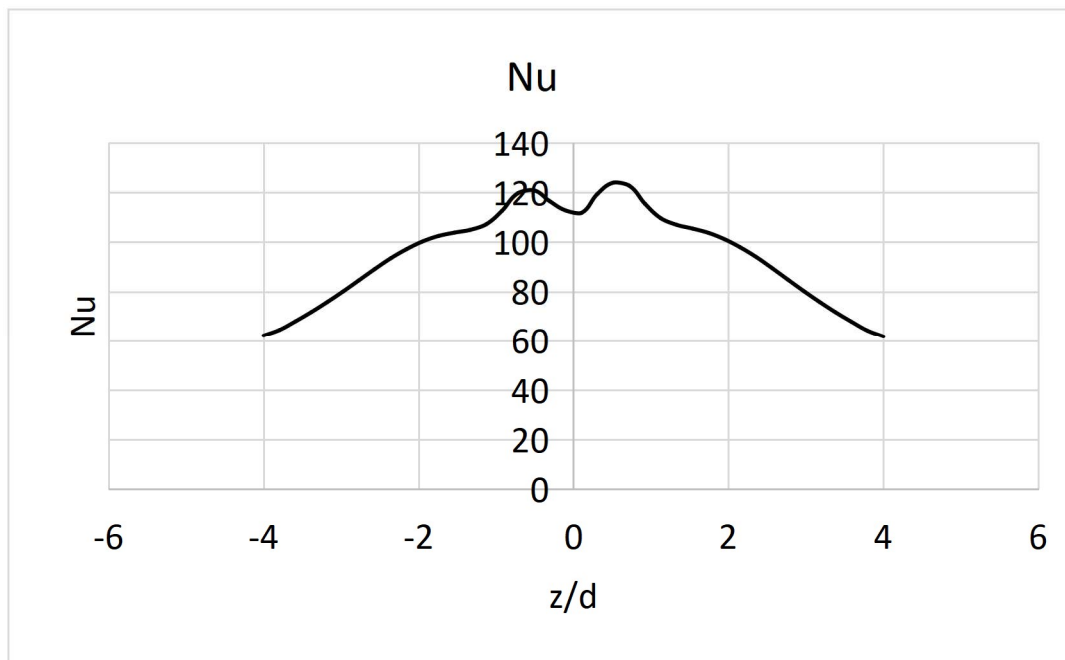


Figure 6.3(g): Nu variation along z/d

Figure 6.3(h) shows a schematic representation of the streamline from the inlet to the wall plate. The convergence of these streamlines at a particular point in the middle of the geometry indicates the nozzle through which the jet flows. The wire frame at the base of the plate represents the entire length of the plate, shown by $L = 8d$ from $-4d$ to $+4d$.

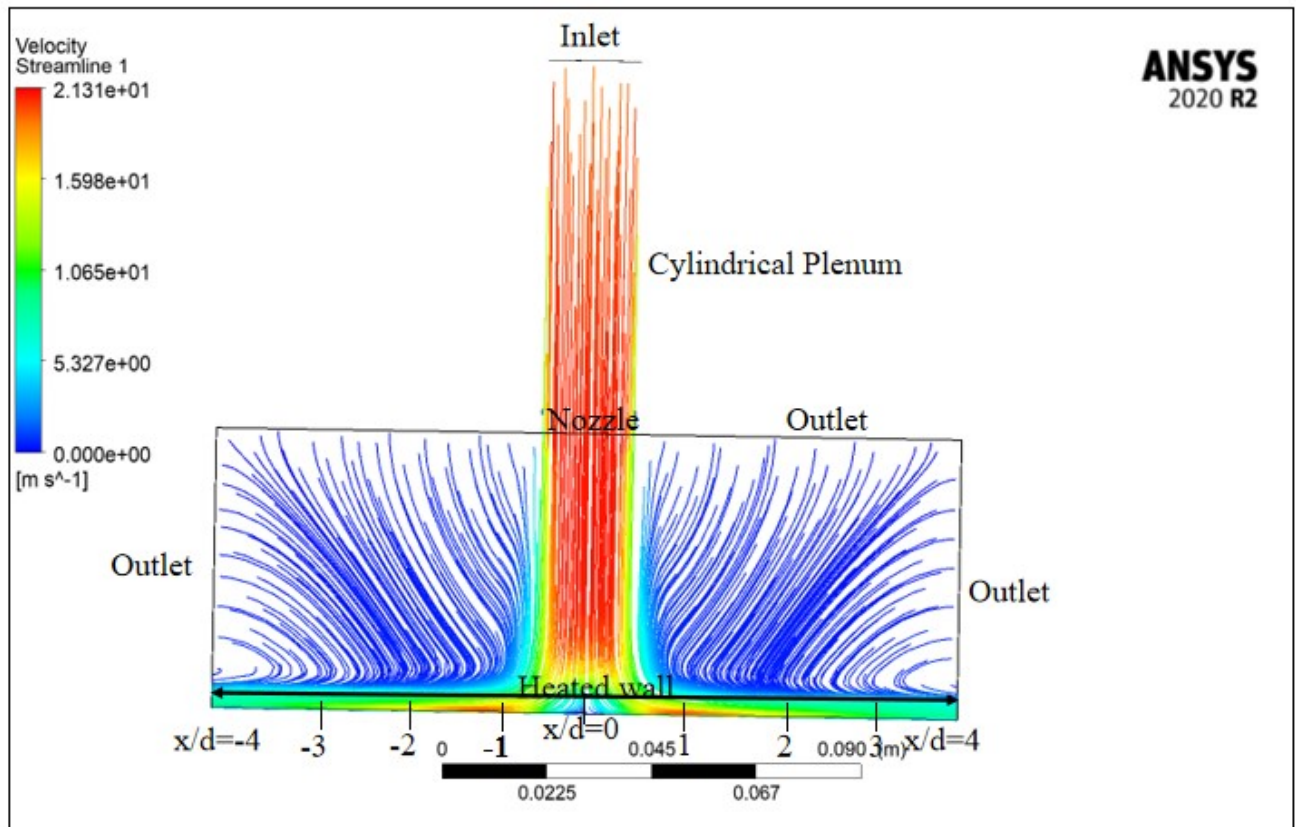


Figure 6.3(h): Streamline is schematically shown with $H/d = 3$.

Even with the same $H/d = 3$, the velocity vectors at the nozzle are crucial in explaining variations in the pressure coefficient. As a result, velocity vectors close to the nozzle region are displayed in Figure 6.3(i).

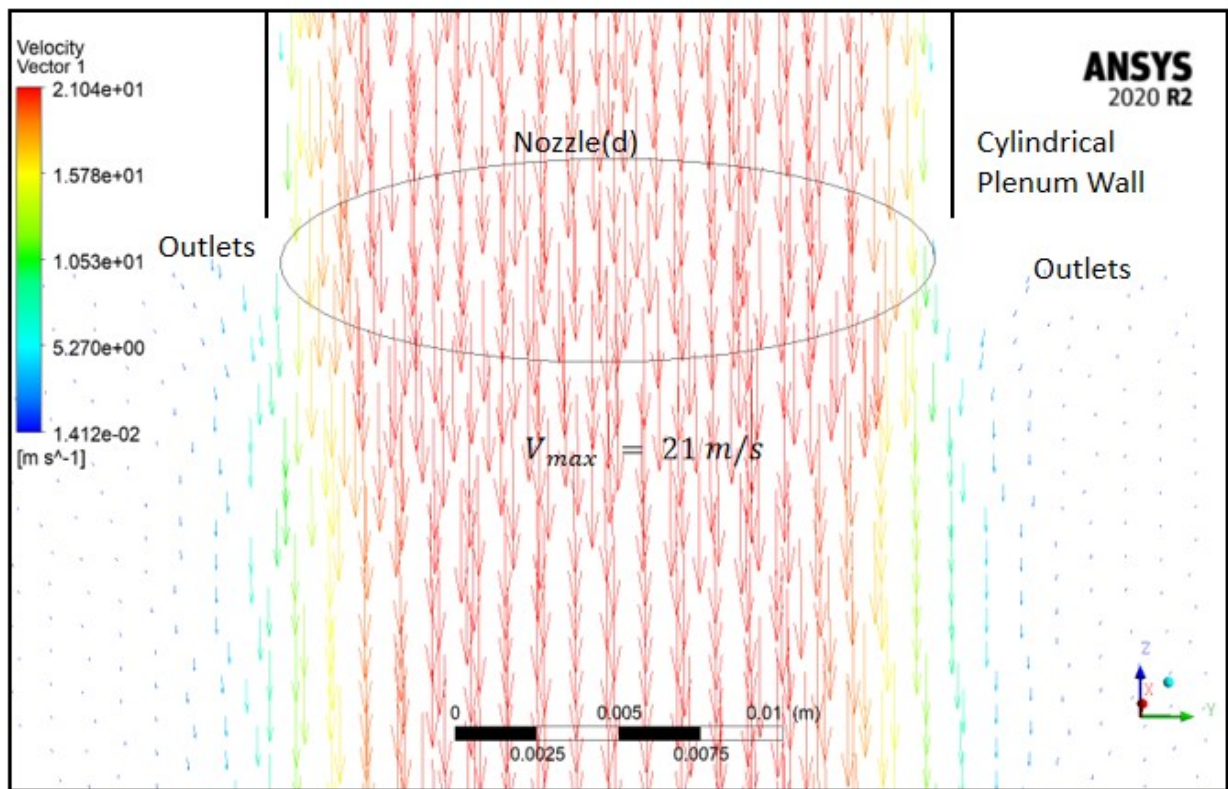


Figure 6.3(i): Velocity vectors near the nozzle. Nozzle diameter (d) and plenum plate thickness is $3d$, the maximum velocity is 21 m/s and the entrance nozzle velocity is 19.31065 m/s

Figure 6.3(j) illustrates the velocity vectors in close proximity to the jet impinging plate. The blue colour of the vectors that are in close proximity to the periphery of the heated wall indicates that there is no slip condition.

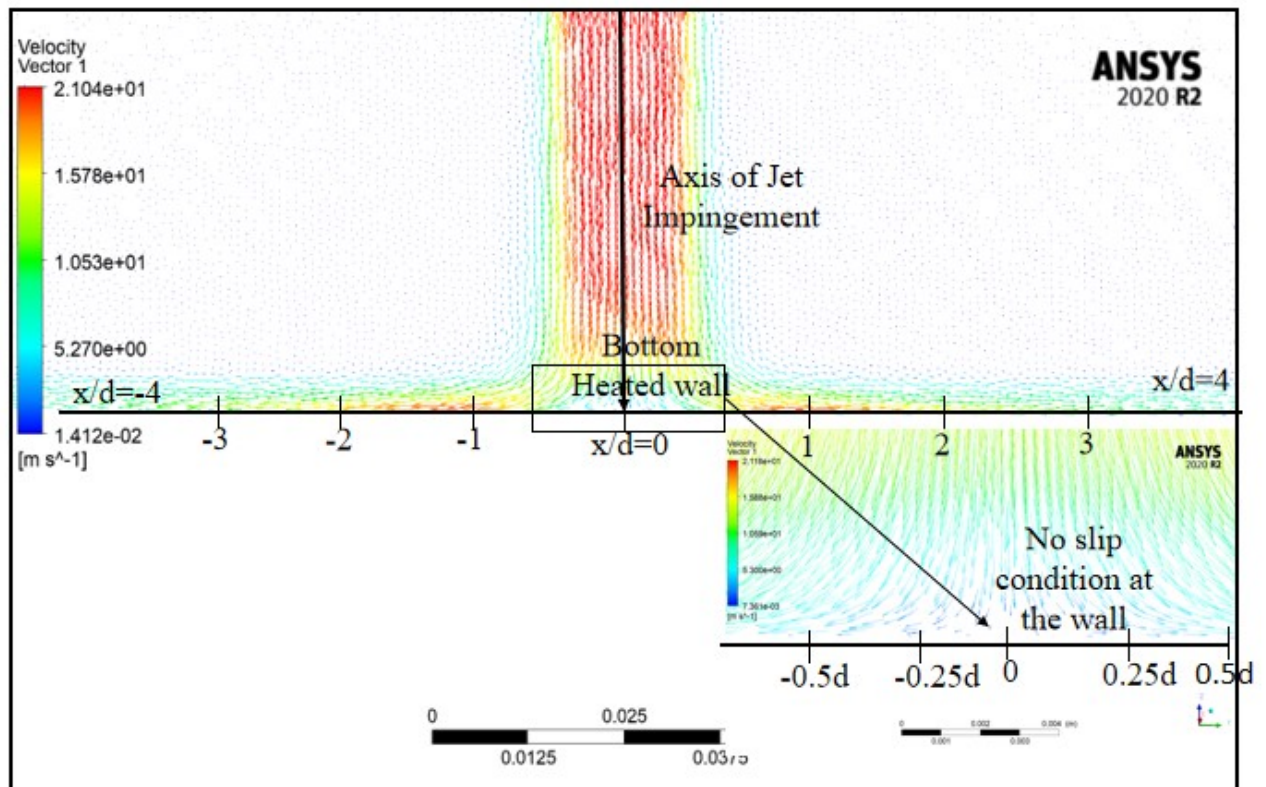


Figure 6.3(j): Vectors close to the heated wall is shown from $x/d = -4$ to $x/d = 4$

7-Conclusions:

The fluid flow and heat transfer processes have been extensively discussed from sections 1 to 6 of this report. The commercially available design software ANSYS FLUENT 2020 Version has been used to perform all the numerical simulations. The first two simulation which includes laminar and turbulent flow through pipe is fundamentally simulated in order to learn the process of simulation in Ansys Fluent. Section 3 of the report is the preliminary testing the result of jet impingement on flat plate from the paper by Kannan B T tittle, ‘Steady State Jet Impingement Heat Transfer from Axis-Symmetric plates without grooves’. Results have been superposed with Kannan’ s results but the results exactly not superposed due to lesser data provided in his reference paper therefore required data has been assumed. Also the simulation performed is 3 d case instead of axis symmetric.

The key portion of the report is to numerically simulate the later simulation from section 4 to 6. The key observation obtained is even with same nozzle velocity and $H = 3d$ in all three simulations the pressure distributions and Nu distributions found to be different. It implies that plenum configuration results in different velocity vector distributions close to the nozzle as shown in figure 4.3(i),5.3(i) and 6.3(i) of the report. Upon thorough examination of the velocity vectors in the vicinity of the nozzle, the reason for this is revealed. The maximum velocity in relation to the nozzle entrance velocity for the cubical plenum covered in section 4 of the report is 26.6 m/s, the maximum velocity for concave plenum configuration is examined in section 5 of the report is 23 m/s and for cylindrical plenum configuration is studied in section 6 at 21 m/s. We may therefore conclude that, despite the fact that the nozzle velocity at the entrance, which is 19.31065 m/s and $H/d = 3$, is the same in all configurations from section 4 to section 6, the velocity vector development in each of the three configurations is different. The C_p thus being highest for cubical plenum. This is obtained at the penalty of it's configuration. The superposed C_p values are shown in figure 7(a) and 7(b).

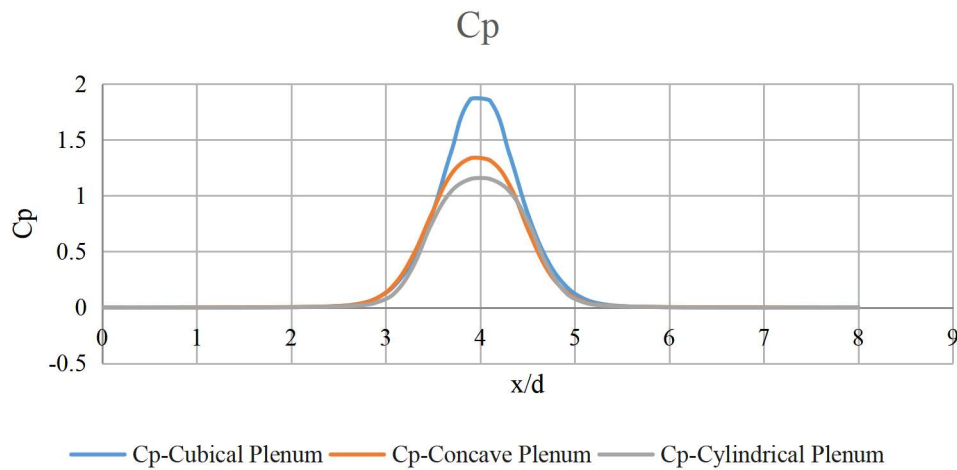


Figure 7(a): Superposed C_p values for all three different plenum configuration is plotted against x/d .

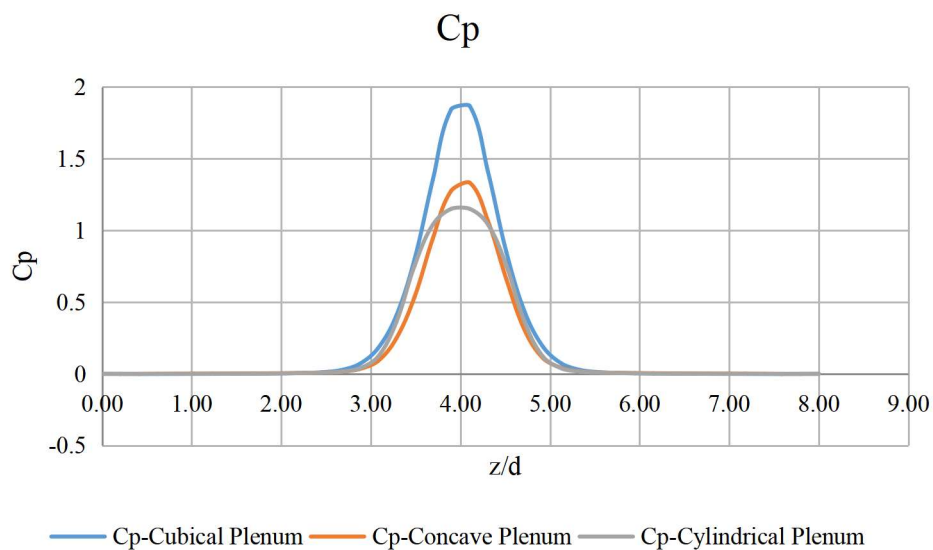


Figure 7(b): Superposed C_p values for all three different plenum configuration is plotted against z/d .

Nu distribution similarly for these 3 plenum configuration is shown in figure 7(c) and 7(d).After analyzing all superposed plots both for pressure coefficient and Nu number one must conclude how plenum chamber configuration plays a key role in pressure distribution.

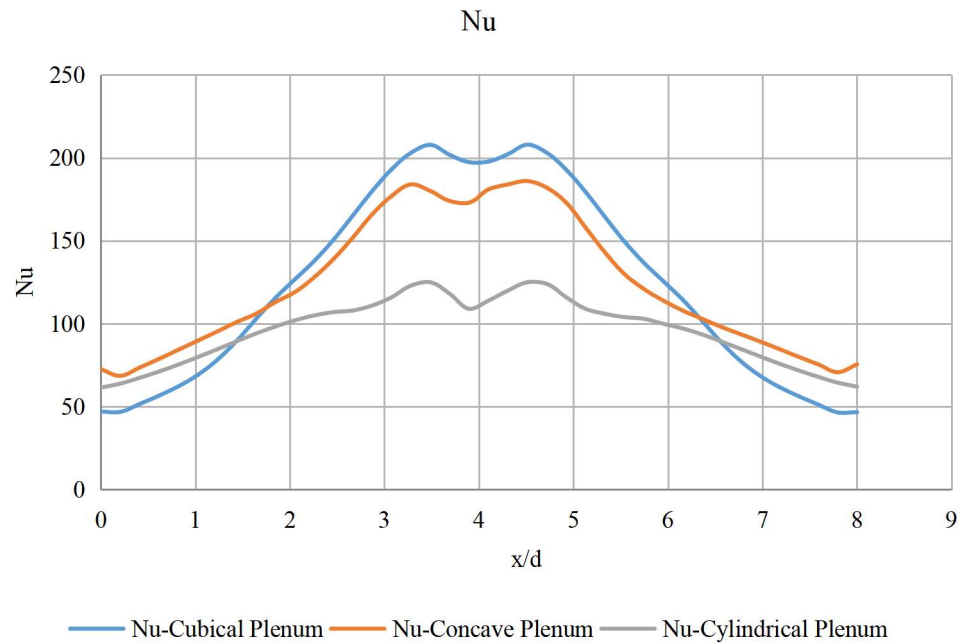


Figure 7(c): Superposed Nu values for all three different plenum configuration is plotted against x/d

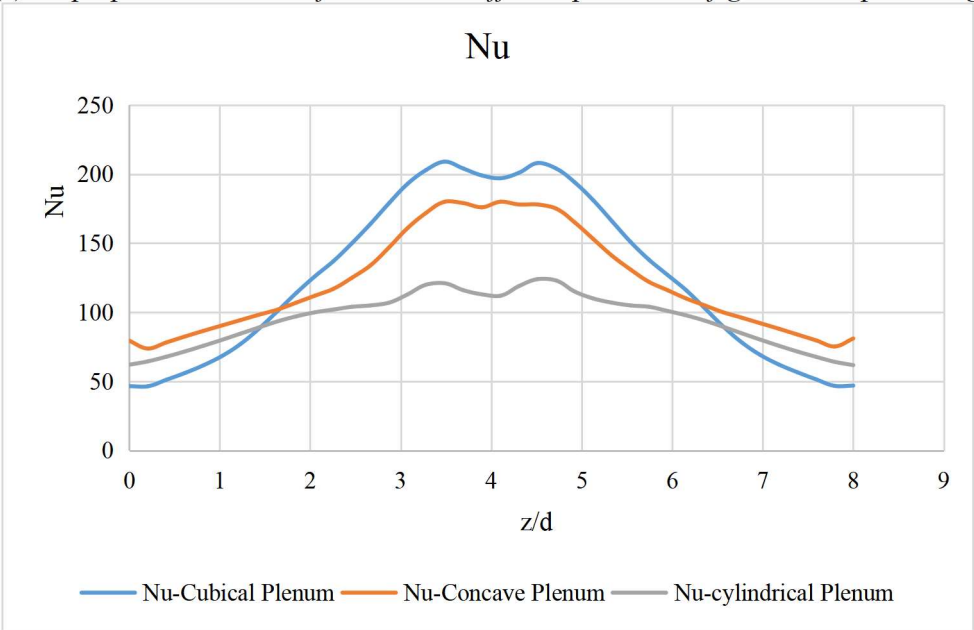


Figure 7(d): Superposed Nu values for all three different plenum configuration is plotted against z/d